

Pore-network study of the mechanisms of foam generation in porous media

Min Chen and Yannis C. Yortsos*

Department of Chemical Engineering, University of Southern California, Los Angeles, California 90089-1211, USA

William R. Rossen

Department of Petroleum, and Geosystems Engineering, The University of Texas at Austin, Austin, Texas, 78712-0228, USA

(Received 28 March 2005; revised manuscript received 13 December 2005; published 6 March 2006)

Understanding the role of pore-level mechanisms is essential to the mechanistic modeling and simulation of foam processes in porous media. Three different pore-level events can lead to foam formation: snapoff, leave behind, and lamella division. The initial state of the porous medium (fully saturated with liquid or already partially drained), as surfactant is introduced, also affects the different foam-generation mechanisms. Bubbles created by any of these mechanisms cause the formation of new bubbles by snapoff and leave behind as gas drains liquid-saturated pores. Lamellae are stranded unless the pressure gradient is sufficient to mobilize those that have been created. To appreciate the roles of these mechanisms, their interaction at the pore-network level was studied. We report an extensive pore-network study that incorporates the above pore-level mechanisms, as foam is created by drainage or by the continuous injection of gas and liquid in porous media. Pore networks with up to 10 000 pores are considered. The study explores the roles of the pore-level events, and by implication, the appropriate form of the foam-generation function for mechanistic foam simulation. Results are compared with previous studies. In particular, the network simulations reconcile an apparent contradiction in the foam-generation model of Rossen and Gauglitz [AIChE J. **36**, 1176 (1990)], and identify how foam is created near the inlet of the porous medium when lamella division controls foam generation. In the process, we also identify a new mechanism of snap-off and foam generation near the inlet of the medium.

DOI: [10.1103/PhysRevE.73.036304](https://doi.org/10.1103/PhysRevE.73.036304)

PACS number(s): 47.56.+r, 47.50.-d, 47.54.-r, 83.90.+s

I. INTRODUCTION

In the petroleum industry, foam is used in porous media for two primary purposes: gas diversion to improve oil recovery [1–3], and acid diversion for matrix acid treatments [4,5]. Foam is also used to direct the flow of remediation fluids in subsurface aquifer-remediation processes [6].

A number of studies find that foam does not alter the relative permeability to flow or the viscosity of the liquid phase that makes up the foam [7–10]. Foam does drastically reduce the mobility of gas, however. The reduction is inversely related to the average bubble size [11–14], i.e., it is directly related to the number of liquid films, or lamellae, that separate gas bubbles, per unit volume of gas in the pore space. Lamellae resist the movement of gas by resisting movement themselves: the resistance arises from the drive by each lamella to minimize its surface area, according to its interfacial tension. Lamellae form in pore throats; thus, initiating movement of a lamella requires pushing it out of the pore throat, which is the position of minimum surface area, into the pore body, a position with larger surface area [12–19]. The pressure drop ΔP^{\min} required to mobilize a stationary lamella is inversely proportional to its minimum radius of curvature, which is of the order of the radius of the pore throat R :

$$\Delta P^{\min} \sim 4\gamma/R \quad (1)$$

where γ is the interfacial tension between liquid and gas.

When lamellae block a relatively small fraction of pore throats, gas continues to flow as a Newtonian fluid, albeit with reduced relative permeability [20,21]. If enough lamellae are present to block continuous gas flow, the gas behaves as though it had a yield stress, because it cannot flow unless the pressure gradient is sufficient to mobilize lamellae along some pathway through the pore network. During this process, much of the gas may remain trapped even as some fraction of the gas flows [10,22–24]. However, the specific mechanism by which this occurs is very much unclear at this point. The pressure gradient required to keep lamellae moving along this path may also be less than that required to initiate flow [13–19]. Initiating flow requires mobilizing all the lamellae along the path from their initial positions in pore throats, where the resistance is greatest. Once lamellae are moving, their average threshold resistance may be less, because most of the time, they are individually in positions of lower resistance. In addition to the effective yield stress, however, the drag on moving lamellae imparts a viscous resistance, typically in the form of a shear-thinning viscosity [11,19]. Viscous effects, although not of the shear-thinning type, will be considered in this study.

Conditions for gas mobilization and flow and the resulting foam mobility depend on the number density of lamellae in the gas phase. The latter depends on processes that create and destroy lamellae, which are in turn influenced by flow. These aspects will be studied here using pore-network simulation. We proceed by providing first a brief literature review of individual lamella generation in single pores. In the analysis to follow, lamella destruction, e.g., by high capillary pressure, especially near the “limiting capillary pressure” [25,26], will not be reviewed. Lamella destruction plays a

*Corresponding author. Email address: yortsos@usc.edu

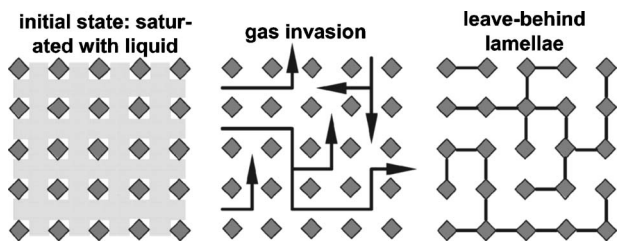


FIG. 1. Schematic of lamella creation by the leave-behind mechanism. Gray diamonds represent sand grains; gaps between them represent pore bodies and throats.

large part in controlling steady-state foam properties, but is not the focus of this paper. When our problem reaches either a steady or an oscillatory state, it is because lamella creation is balanced by transport of lamellae out of the network.

A. Lamella-creation mechanisms

It is commonly accepted that lamellae are created by the following three mechanisms [2,14,27,28].

(i) “Leave behind” is creation of stabilized liquid films or lenses in pore throats as gas invades adjacent pore bodies through other throats, e.g., as illustrated in Fig. 1. The presence of surfactant is necessary for lamella stabilization. Depending on pore-throat geometry, leave-behind lenses may break, if surfactant is not present. Although sometimes cited as a source of “weak” or ineffective foam [10], the leave-behind mechanism can create a large number of lamellae [2]. However, if it is the only lamella-creation mechanism, the gas will always have at least one continuous pathway for flow.

(ii) “Lamella division” denotes the event when two or more lamellae are created from a single one. Each time a mobilized lamella passes a pore body, with more than one pore throat unoccupied by liquid or another lamella, this must either break or span both open throats, e.g., as illustrated in Fig. 2. Lamella division can result in the filling of a large region of the pore space with lamellae, starting with only a small number of moving lamellae, e.g., as illustrated in Fig. 3. Models based on the concept of lamella division explain a variety of foam-generation data [20,29–32]. If lamella division were the only mechanism operating, a paradox would afflict this explanation, however: if lamellae must be moving to divide, and presumably they are moving downstream, then how are lamellae created upstream? Should there not be a growing region near the inlet with few lamellae and high gas mobility?

(iii) “Snapoff” is a third mechanism for lamella generation: lamellae are created in gas-filled pore throats (Fig. 4), if

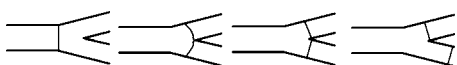


FIG. 2. Schematic of a single lamella-division event. In the first two panels, lamella enters branching point (pore body). Note that two throats are unoccupied by lamellae. In the second two panels, lamella divides in the two downstream throats, creating one additional lamella.

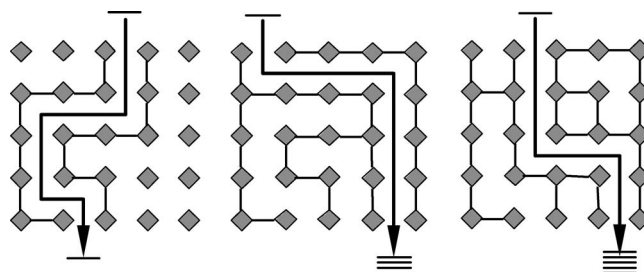


FIG. 3. Schematic of lamella division on the pore-network scale. In the first panel, one moving lamella produces 14 lamellae in place by division. In the second panel, a second moving lamella (taking a different path) produces nine more in place, plus displaces an extra two moving ahead of it. In the third panel, a third moving lamella (taking a different path) produces two more in place, plus displaces an extra five moving ahead of it.

the local capillary pressure falls to about half the capillary entry pressure of the throat [2,13,33]. [While it depends on the geometry of the throat and the wettability of the medium, the value of one-half is a reasonable representative value for three-dimensional (3D) pore geometries.] A paradox is also associated with the snapoff mechanism. If gas occupies the throat, then the capillary pressure is (or was) at the capillary entry pressure. How does capillary pressure at the throat fall to one-half this value to trigger snapoff? There are seven ways by which this can happen [33]. Three are relevant to steady flow in homogeneous media and to the discussion that follows.

(1.) Capillary pressure fluctuates as moving lamellae shift their positions and curvatures, altering the pressure drop between bubbles.

(2.) Since gas is nearly inviscid, the pressure is nearly uniform along gas bubbles. Therefore, the capillary pressure is lower at the rear of long bubbles than at the leading edge.

(3.) When gas invades a wide liquid-filled pore body through a narrow pore throat, liquid draining from the pore body can sweep back into the throat and cause snapoff, as illustrated in Fig. 5. This is commonly called “Roof snapoff” after Roof’s study of oil trapping in water flooding [34].

In Roof snapoff, alone among snapoff mechanisms, the size of the pore body relative to the throat matters, because it is its radius that briefly controls local capillary pressure at the moment gas fills the pore body. Some, but not all, pores then become “germination sites” for lamella creation [14,27] but only when gas invades a pore body filled with liquid. In all other snapoff mechanisms, snapoff depends on the radius of the throat alone (and the local capillary pressure).

B. Models for foam generation

Continuum models used in foam process simulation in porous media are generally empirical. Thermodynamic and



FIG. 4. Schematic of snapoff in a pore throat. Black denotes pore-throat wall, gray water, and white gas.

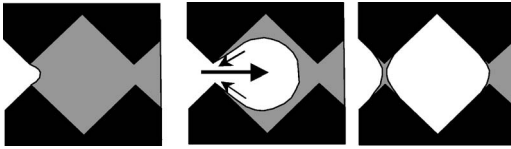


FIG. 5. Schematic of Roof snapoff as gas invades a pore body. Black is pore wall, gray is water, and white is gas.

flow properties are approximated by empirical models based on the lamella density per unit volume. Rates of lamella generation are postulated based on averaging over the pore network. A number of foam-generation models are based on the assumption of repeated Roof snapoff, long after the pore body drains its liquid [14,21,35–43]. In particular, “break and reform” models [21,39–43] assume that lamellae form by snapoff in pore throats, are mobilized, immediately break upon mobilization, and then, after a short delay, reform by snapoff. Rossen [33] reviews the evidence for this assumption and shows that it is problematic. These models do not explain why liquid would drain back to the throat at high capillary pressure, or how capillary pressure could be low enough to trigger liquid flow to the throats.

Other models for creation of strong foam (i.e., foam of very low gas mobility, thought to reflect a discontinuous gas phase) are based on mobilization and division [20,29,31,32]. Rossen and Gauglitz [20] presented a model to explain the minimum velocity (or pressure gradient) required to create strong foam in a porous medium already partially drained by gas before surfactant was introduced. This is a fundamental property for foam flow in porous media. They assumed that some fraction of the pore throats are occupied by liquid before foam is created. Once surfactant is present and injection rates increased, lenses drain to lamellae, which can be mobilized, if pressure drop across the lamella is sufficient [see Eq. (1)]. The lamellae first mobilized would be those that block large stagnant gas clusters from flowing. The local pressure drop required to mobilize an individual lamella is related to the macroscopic pressure gradient $|\nabla P^{\min}|$ and the length of the gas cluster L_c containing the lamella:

$$\Delta P^{\min} = |\nabla P^{\min}| L_c. \quad (2)$$

Equation (2) implicitly assumes that the pressure gradient is uniform across the pore network. Using percolation theory in a Bethe tree network, Rossen and Gauglitz [20] derived an explicit formula for the average cluster size as a function of the nearness to the percolation threshold. The size diverges to infinity as the percolation threshold is approached, where therefore foam generation becomes easier. Because one can also relate the nearness to the percolation threshold to the injected liquid-gas volume ratio and fluid viscosities, one can predict the minimum pressure gradient $|\nabla P^{\min}|$ from the injected liquid fraction. Rossen and Gauglitz [20] showed good agreement of their model with the data, after adjusting one parameter accounting for the number of lamellae that must be mobilized to trigger foam generation. The model predicts that $|\nabla P^{\min}|$ varies inversely with permeability, for porous media with scalable pore geometry, like sandpicks and bead-

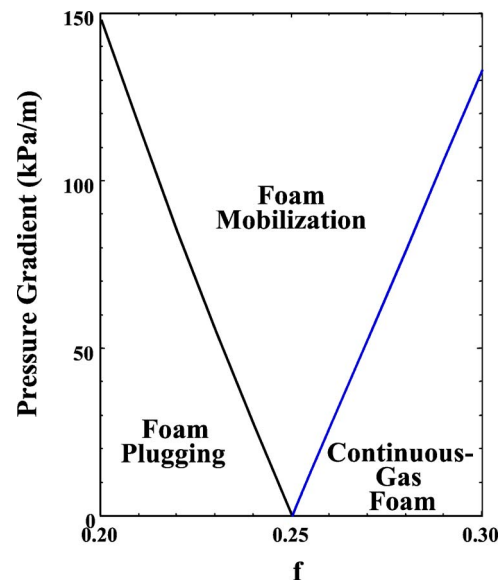


FIG. 6. (Color online) Schematic of the results of the percolation model for foam generation by Rossen and Gauglitz. f is the fraction of pore throats through which gas can flow (not blocked by water-filled pores, lenses, or lamellae). Here $f=0.25$ represents the percolation threshold, where the pressure gradient for foam mobilization $|\nabla P^{\min}|$ approaches zero. The diagonal line on the right side of figure represents foam generation during continuous injection of gas and liquid (starting from no-foam state of continuous gas flow). The diagonal line on the left side of the figure represents mobilization of discontinuous-gas foam.

packs. The data of Gauglitz *et al.* [30] confirmed this prediction.

Rossen and Gauglitz [20] proposed a similar model when the gas is discontinuous, but still assuming that the lamellae are placed randomly in the pore network, as in percolation theory. Like the version for continuous-gas foams, $|\nabla P|$ is assumed to be uniform across the pore network. For discontinuous-gas foams, the mobilization pressure gradient approaches zero at the percolation threshold, because the average bubble size approaches infinity there. The complete results of the model are shown schematically in Fig. 6.

Rossen *et al.* [44] relaxed several simplifying assumptions made in the Rossen and Gauglitz [20] model. First, an improved estimate of $|\nabla P^{\min}|$ for mobilizing discontinuous-gas foams in a Bethe tree network gives some curvature to the straight line to the left of the percolation threshold in Fig. 6. In addition, for continuous-gas foams, Rossen *et al.* [44] recognized that while the average cluster of gas blocked by a lamella diverges to infinity at the percolation threshold, the number density of these clusters on the pore network approaches zero [45]. The number of clusters greater than any given size goes through a maximum before falling to zero as the percolation threshold is approached [46]. The implications of these two changes in the earlier theory are shown in Fig. 7. The two parts of the model no longer agree at the percolation threshold. Rossen *et al.* [44] contend that the reason for this divergence is that the theory still assumes a uniform $|\nabla P|$ on the pore network near the percolation threshold, which is known not to be valid. Advancing the

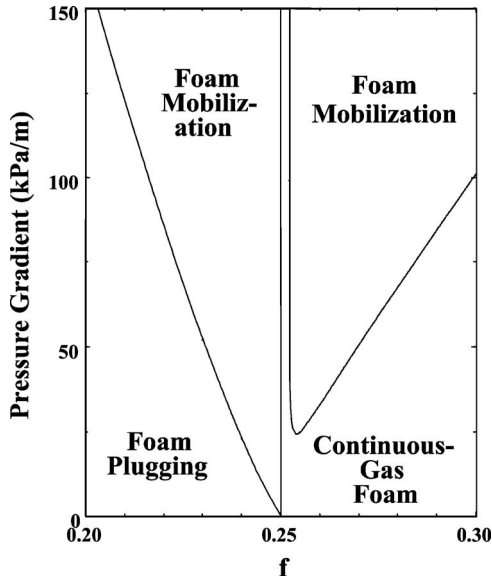


FIG. 7. Schematic of results of the percolation model of Rossen *et al.* [44] modified from that of Rossen and Gauglitz [20]. The two halves of the model diverge from each other at the percolation threshold ($f=0.25$).

theory, and reconciling the two halves of the model, will require a study on a pore network where many of these assumptions can be relaxed. Such a study is reported in this paper.

Tanzil *et al.* [29] examined foam generation upon gas injection into a medium saturated with surfactant solution. They proposed that foam generation depends on exceeding the critical pressure drop across the displacement front rather than on the pressure gradient. They also proposed a critical value of the capillary number based on the pressure drop across the displacement front to denote the threshold of foam generation. An experimental verification of this condition is difficult in fixed-injection-rate experiments, however, because the pressure drop increases upon foam generation. The measured pressure drop is as much a reflection as a cause of foam generation.

C. Purpose of the present study

We noted that foam simulators require expressions for lamella creation. Moreover, in some applications, foam generation itself is in doubt, while the issue of foam generation is crucial to process success. Therefore, it is important to understand foam generation at the pore-network level, a task yet to be reported in the literature. This is the main motivation for the present study. We model on a pore network the three processes of lamella creation (leave behind, lamella division, and snapoff), under various scenarios and flow conditions. The dynamics are complex. For instance, even upon steady flow, once strong foam forms (perhaps by mobilization and division), gas mobility falls abruptly, gas drains additional pores, and additional lamellae are created by snapoff and leave behind, thus leading to an oscillatory state. Using a repetitive snap-off model we probe the validity of the model of Rossen and Gauglitz (cf. Fig. 7). For com-

parison, we show results based on an assumption of repeated Roof snapoff, but by illustrating foam generation by other mechanisms we probe the assertion that repeated Roof snapoff is not necessary for foam generation. Finally, we identify an additional mechanism of snapoff near the pore network entrance, which explains how lamellae are created near the entrance when foam is generated by lamella mobilization. For all these foam-generation scenarios we report relevant thermodynamic and rheological properties.

II. THE PORE-NETWORK MODEL

Modeling foam formation and propagation in a pore network must borrow from two different areas: the flow of two immiscible fluids, where capillary and viscous forces are important, and the flow of a fluid exhibiting a yield stress, for example, of a Bingham plastic. Significant progress has been made in the first area in the last two decades using pore networks (e.g., see the recent review by Blunt *et al.* [47]). Modeling the onset and subsequent flow of a Bingham fluid, however, has only recently been accomplished (Chen *et al.* [48]). A key tool for solving the latter problem is the process of invasion percolation with memory (IPM), introduced by Kharabaf and Yortsos [49] to model the onset of flow of a fluid with yield stress. It was recently extended by Chen *et al.* [48] to account for dynamic flow effects following the onset of flow. In the following, we will provide a brief summary of the methods used in the latter study, as they will be repeatedly used in the present analysis.

Consider the flow of a yield-stress fluid in a single pore, denoted by index i , and assume for simplicity the following flow rate–pressure drop relationship across the pore:

$$|q_i| = r_i^4 \left(1 - \frac{1}{|\Delta p_i| r_i} \right) |\Delta p_i| \quad \text{when } |\Delta p_i| > \frac{1}{r_i};$$

$$q_i = 0 \quad \text{when } |\Delta p_i| < \frac{1}{r_i}. \quad (3)$$

This equation states that for flow to occur in pore i , the pressure difference across the pore must exceed a threshold, taken here as $1/r_i$, which depends on the throat size. Following the onset of flow, the flow rate varies in proportion to the departure of the pressure from its minimum, according to a simple Poiseuille-flow expression. (No shear-thinning effects are assumed in that regime.) In Eq. (3), we have used the following dimensionless notation:

$$q = \frac{2\mu_g}{\pi\gamma R^{*2}} Q, \quad p = \frac{R^*}{4\gamma} P, \quad r_i = \frac{R_i}{R^*}, \quad (4)$$

where capital letters denote dimensional and lower case letters dimensionless quantities, Q denotes volumetric flow rate through the pore, R^* is a characteristic pore throat radius (taken as the mean throat radius), and μ_g is the gas viscosity (in the absence of foam). In this notation, which will also be used in the rest of the paper, the threshold in Eq. (3) is the dimensionless analog of Eq. (1), and it is inversely proportional to the pore radius. The characteristic flow rate in Eq. (4), namely, $\pi\gamma R^{*2}/2\mu_g$, is that which would result from the

application of a pressure gradient equal to $4\gamma/R^*$.

Consider, now, mobilization and flow driven by a pressure difference applied across a network of pores. Clearly, for flow of the yield-stress fluid to occur, a minimum overall threshold must first be exceeded,

$$\Delta p^{\min} = \min_i \sum \frac{1}{r_i} \quad (5)$$

where the summation is over all throats over a connected path across the sample. Determining the onset of flow in a pore network with distributed thresholds is not a trivial task. It was analyzed in detail by Kharabaf and Yortsos [49] who showed that there exists a specific path, the minimum threshold path (MTP), over which the corresponding sum of thresholds is minimum. Key to their analysis was the development of a method, termed invasion percolation with memory, which extends standard invasion percolation theory [50]. Details on IPM are given in Ref. [49]. Here we will simply note that for a uniform distribution of thresholds in the range $[0, 1]$, the minimum pressure gradient is about 0.3 for a 2D square lattice [49]. In the present case of a uniform distribution of radii in the range $[0.5, 1.5]$, the corresponding value for a 2D lattice is found to be about 0.96. IPM forms the backbone of the present algorithm as well and will be repeatedly used below.

The IPM algorithm defines the minimum threshold path, given a specified arrangement of thresholds. The subsequent opening of new paths, at higher pressure difference, cannot be strictly determined by a static application of IPM alone, however. Following the onset of flow, viscous effects become important and need to be added to the thresholds, and the algorithm for opening new paths must be modified. Now, opening a new path is determined not only by the capillary threshold $1/r_i$, but also by the global velocity field, which affects the pressure distribution along the mobilized paths and contributes additional resistance. Thus, even though the first path to be mobilized is indeed the MTP, identified using IPM, finding the subsequent fraction of the mobilized fluid requires a more elaborate iterative approach. Chen *et al.* [48] solved this problem by using updated dynamic thresholds, which depend on the flow rate. Thus, the updated dimensionless threshold τ_k of a throat k in a flowing path becomes

$$\tau_k = \frac{q_k}{r_k^4} + \frac{1}{r_k} \quad (6)$$

where q_k is the corresponding flow rate through that throat. The new paths to open at any incremental pressure above the minimum can still be determined using IPM, but now with all thresholds in the flowing part updated following Eq. (6). The process works incrementally, by determining successively at small increments of the applied pressure drop the corresponding conducting paths. In doing so, paths determined at the prior step always remain minimum paths at the next increment. An iterative algorithm is needed for convergence. Calculation details are found in Ref. [48].

To determine the pressure distribution due to viscous flow, and hence the flow rates needed to update the thresholds in Eq. (6), we assume incompressible fluids, and use Eq. (3) (or

any other appropriate local expression) for the momentum balance. A mass balance for any site i along the flow path then gives

$$\sum_j^Z q_{ij} = 0 \quad (7)$$

where q_{ij} is the volumetric flow rate from site i to its neighbor site j , and Z is the coordination number of the lattice (e.g., $Z=4$ for a square or -6 for a cubic lattice). The resulting equations for pressure were solved using a combination of conjugate gradient and successive over-relaxation methods. Because of the inherent nonlinearities of the problem, the algorithm is time consuming, thus limiting the networks studied to relatively small sizes. For this reason, some finite-size effects may exist in the results reported below.

When the yield-stress fluid is not a Bingham plastic, but rather a continuous or discontinuous gas phase in the presence of dynamically evolving foam lamellae, additional complications arise due to the fact that the positions of lamellae, which dictate the mobilization thresholds, are not fixed [15–19]. Rather, these constantly vary, as a result of both movement of lamellae and their generation and destruction. Rates of generation depend on the flow and pressure distribution, resulting in a complex, dynamic, and nonlinear problem. Lamella generation is incorporated by the mechanisms of snapoff, division, and/or leave behind, as appropriate, but lamella destruction was omitted, as noted above. The calculation of the minimum pressure gradient, which is an important thermodynamic and flow variable, is obtained by solving the fluid-flow problem in the continuous gas phase, along with the use of IPM, when the gas phase is continuous, and by applying IPM only, when the gas phase is discontinuous. Although quite important, the effect of the pore-size distribution was probed in only two cases, one in which the size distribution was unimodal (dimensionless pore size equal to 1) and another in which it was uniform in the range $[0.5, 1.5]$. The relevant dimensionless parameters are the capillary number $Ca \equiv Q_w \mu_w / \gamma$, the viscosity ratio $M = \mu_w / \mu_{nw}$, the Roof snapoff probability f_s (see below), and the dimensionless capillary pressure, where appropriate. Subscript w refers to the aqueous liquid phase. The sensitivity of the results to several of these parameters is reported below. Note that the capillary number as defined here is based on velocity and viscosity of the liquid and does not reflect the state of foam generation.

In the following sections we will consider various scenarios of foam generation under different conditions. The differences between scenarios concern how lamellae are generated, e.g., by repetitive Roof snapoff, by Roof snapoff during drainage only, or by capillary-pressure fluctuations. We will focus on foam states corresponding to incipient mobilization, namely, where the system is always at conditions of minimum pressure gradient for mobilization, as well as on states corresponding to a fixed applied pressure gradient. The first case yields important thermodynamic and flow properties at the onset of flow. If the gas phase is discontinuous, this corresponds to an experiment with gas injection at a fixed, very low velocity. The second case, at fixed pressure

gradient, sheds light on the foam rheology. Three different cases will be explored. Case I involves lamella generation with repetitive Roof snapoff at germination sites, effectively corresponding to conditions of strong foam. Case II relaxes the assumption of repetitive snapoff and introduces lamella generation by capillary fluctuations. Finally, case III involves the simultaneous steady-state flow of liquid and gas, with lamellae generated by flow displacement.

III. RESULTS

A. Case I: Repetitive roof snapoff at germination sites

The first case studied involves repetitive snapoff of lamellae in specific germination sites, randomly distributed in the pore network, with probability (the snapoff probability) f_s . This scenario mimics lamella generation following the Roof snapoff criterion, and has been frequently postulated [10,14,21,35–43]. For example, it was used in a previous mechanistic pore-network study to model foam invasion in a porous medium [43]. Its key feature is that as lamellae are mobilized from fixed germination sites, new lamellae are instantly generated there to replace them. The liquid does not affect the process other than by supplying the small amount needed to form lamellae. Given that lamellae are constantly generated, a strong foam is expected. The state of the foam depends on the applied pressure gradient. As discussed, two different states were considered: (i) The foam state is determined by sequentially applying the minimum pressure gradient required to mobilize at least one lamella (state of incipient mobilization); (ii) the foam state is determined by the application of a fixed pressure gradient higher than the minimum. In either event, the history of the process is expected to affect the final outcome.

The mechanism of repeated Roof snapoff after the pore body drains of liquid is problematic and probably not realistic [33]. However, assuming repeated Roof snapoff allows a comparison with the cases to be examined later, while as shown below it also maps roughly on to the assumptions of the foam-generation model of Rossen and Gauglitz [20].

1. State of incipient mobilization (minimum pressure gradient)

In this scenario, lamellae are initially distributed in the throats (germination sites) of the pore network according to probability f_s . The gas phase may or may not be continuous, depending on the value of f_s (percolation theory for a 2D square lattice would suggest the condition $f_s < 0.5$ for a continuous gas, but this case is more complex). The algorithm implemented determines the minimum pressure gradient to mobilize at least one lamella, following which event new lamellae are generated by lamella division. When a mobilized lamella leaves the germination site, a new lamella is automatically created to replace it at the same site. The minimum pressure gradient to mobilize the first lamella in the new state is calculated and applied across the network, following which lamellae are mobilized, new lamellae are generated, etc. Mobilized lamellae at the exit end leave the pore network; therefore we anticipate that an asymptotic state will

be ultimately reached even though no lamellae are destroyed. (In a slightly different version of the same scenario, lamellae that left the exit end were reintroduced at the entrance, in a periodic-boundary-condition scheme. The differences from the case presented were found to be minimal, however.) An interesting question is the nature of this state of incipient mobilization, namely, whether it is steady, oscillatory, or random.

Typical results for this scenario are shown in Figs. 8–10 corresponding to different snapoff probabilities f_s for the case of a pore-size distribution uniform in the interval [0.5,1.5]. Note that the pressure drops reported here do not represent pressure drops that would be measured in a laboratory experiment at fixed injection rate. Rather, they denote the minimum value required to mobilize a lamella in the pore network. If the gas phase is continuous, and the actual pressure drop is less than this value, gas flows with no lamella mobilization. If the gas phase is discontinuous, and the actual pressure drop is less than this value, the gas phase will not flow. These results illustrate the dynamics of the minimum pressure drop for mobilization, but not the actual observable pressure drop at a specific flow rate. Figure 8(a) shows the minimum pressure difference as a function of the state of the foam. Figure 8(b) shows the corresponding numbers of lamellae generated by snapoff, lamella division, and leave behind. They both correspond to $f_s=0.2$. In this case mobilization does not lead to strong foam. The figures show that after about 200 steps, the system locks into a periodic state. While the number of snapoff lamellae rises only slightly above its initial value, the number of lamellae generated by division and leave behind increases significantly, as a result of lamella mobilization. The minimum pressure gradient ultimately reaches a state fluctuating, in dimensionless notation, between about 0.17 and 0.02, with a rather intricate pattern in between, as explained below. In this case of low snapoff probability, the fluctuation is periodic (with a period of 13 for the specific case of Fig. 8). Figure 8(c) shows snapshots of the initial state and of one of the final states. While the generation of additional lamellae is evident, the gas phase is still continuous. The bottom panel in Fig. 8 shows schematically the path being mobilized. It consists of a “lamella streamtube” [a schematic of which is shown in Fig. 8(d)] containing a train of lamellae, the sequential mobilization of which follows the pressure gradient fluctuations. Essentially, the system ultimately settles into a pattern in which all but the lamellae along the path depicted in the figure remain stationary. The fluctuating pressure gradient reflects the following mechanism: The mobilization path is “shielded” on all sides by lamellae that are stationary, or are generated by division as a mobilized lamella moves downstream [see Fig. 8(d)], namely the path is essentially a lamella conduit or lamella streamtube. The fluctuating pressure drop is due to the fact that as lamellae move to new locations they encounter pore throats of different sizes, hence of different thresholds, and different overall minimum pressure gradients.

Figure 9 shows corresponding results for a higher snapoff probability $f_s=0.7$, where in both the initial and the final states the gas phase is discontinuous. As the gas phase is discontinuous at all times, strong foam is generated. The

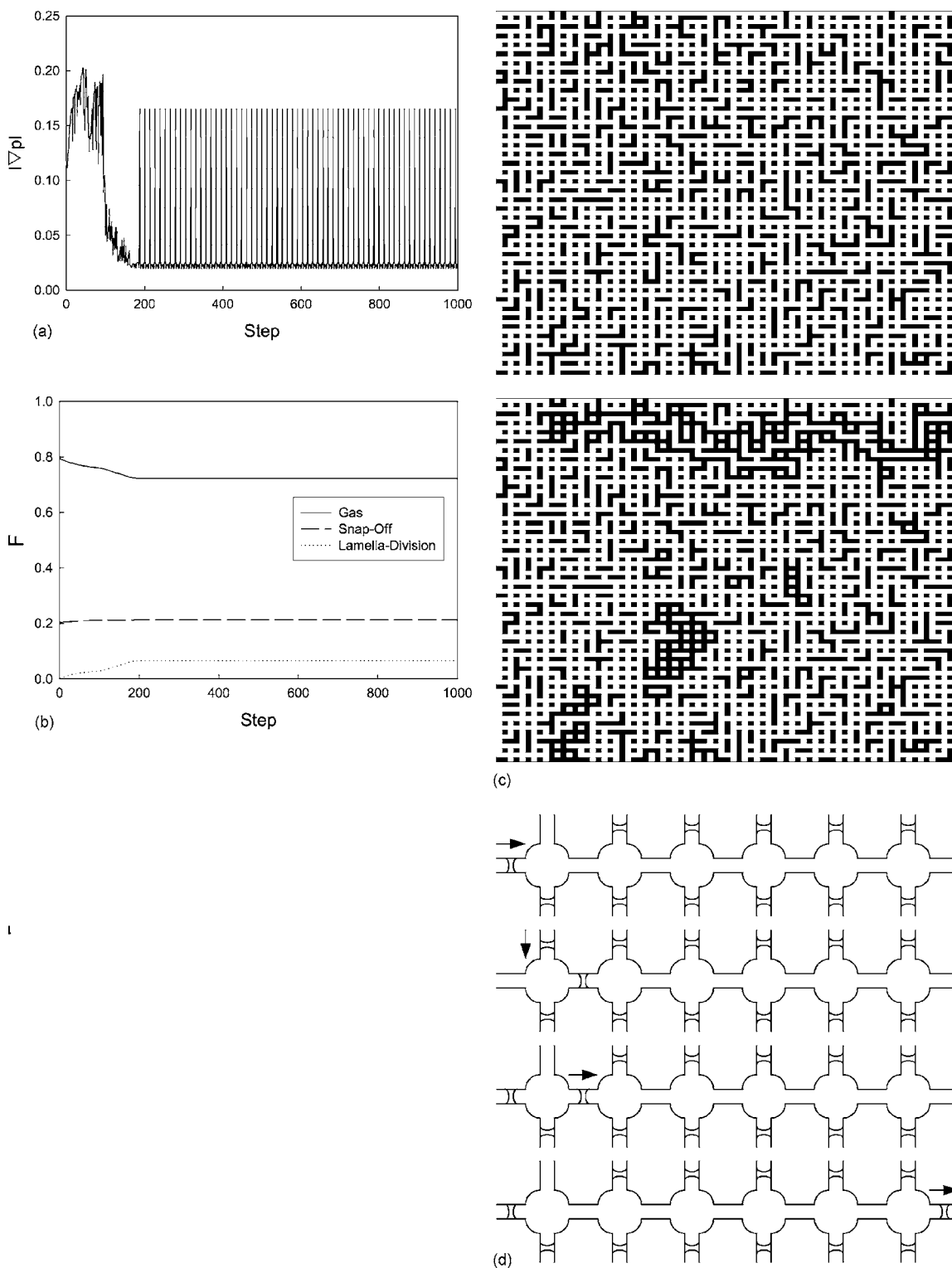
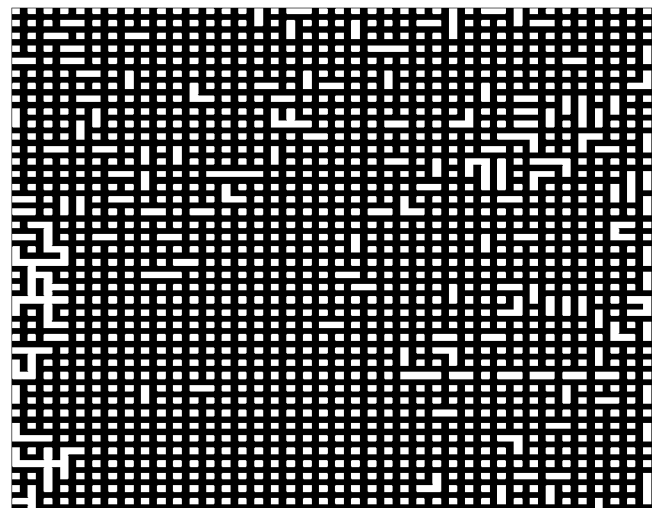
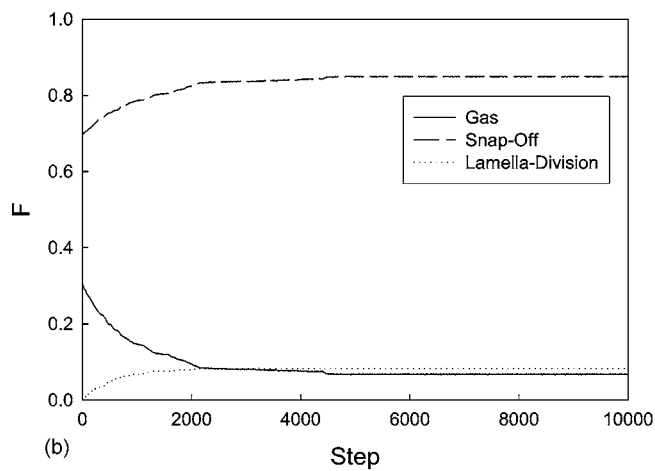
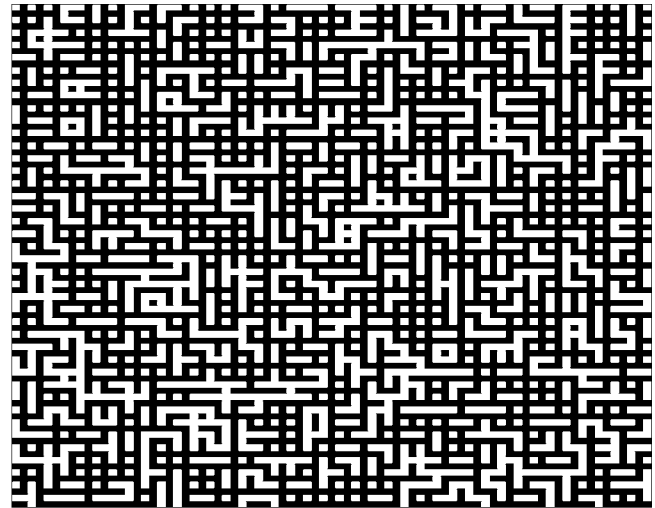
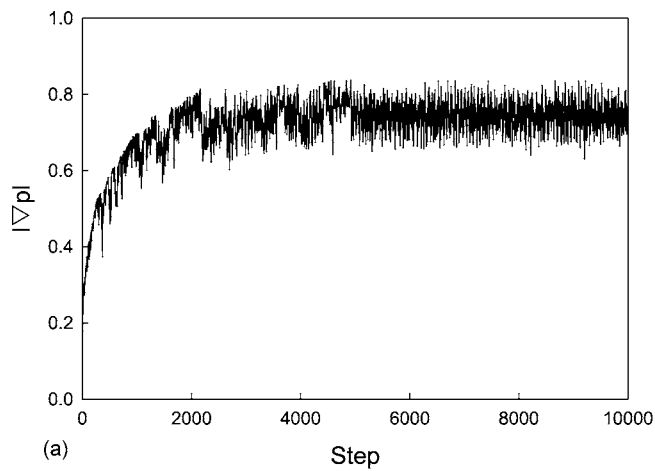


FIG. 8. Foam generation by repetitive snapoff at germination sites ($f_s=0.2$, uniform pore-size distribution). (a). The minimum pressure gradient corresponding to the state of incipient mobilization. The gas is continuous in all states. (b) The fraction of pore throats occupied by continuous gas or lamellae of various types. The gas is continuous in all states. (c) Two lamella patterns corresponding to the initial state and one of the final states of (a). The gas is continuous in all states. (d) Simplified schematic illustrating the concept of a lamella streamtube. The arrows indicate the mobilized lamellae and the direction in which they are mobilized. In the first panel, the moving lamella divides into two unoccupied downstream throats. In the second panel, the mobilized lamella moves to the throat on the left. In the third and consecutive panels (not shown here for simplicity), the lamella moves in the direction of the arrow and occupies consecutive pores without any new lamella generation. The pressure gradient fluctuates as a result of the fluctuating pore size. In the fourth and last panel, the lamella exits the system, thus recreating the top panel. This cycle is then repeated.



(c)

FIG. 9. Foam generation by repetitive snapoff at germination sites ($f_s=0.7$, uniform pore-size distribution). (a) The minimum pressure gradient corresponding to the state of incipient mobilization. The gas is discontinuous in all states. (b) The fraction of pore throats occupied by continuous gas or lamellae of various types. The gas is discontinuous in all states. (c) Two lamella patterns corresponding to the initial state and one of the final states of (a). Gas is white, liquid and rock grains are black.

densities of snapoff lamellae and of lamellae created by division increase with the number of steps. Here it takes a much higher number of steps to reach the asymptotic state, compared to the case of low snapoff probability. As with the previous, the asymptotic state is fluctuating, but now in an apparently random manner. It is of interest that many times the number of the lamellae in the system is mobilized as this fluctuation regime is spanned. A chaotic analysis of the time series showed that the sequence is random, without apparent structure [51]. The fluctuation reveals a rather complex sequence of lamella mobilization and division. Different values of the snapoff probability tried showed the same type of behavior, with lower values of f_s leading to a continuous gas phase and an oscillatory behavior, and with higher f_s leading to discontinuous gas and a random fluctuation.

Figure 10(a) plots the minimum pressure gradient at the asymptotic state (i.e., that which is sufficient to maintain mobilization indefinitely) as a function of $1-F$, where F is the final fraction of throats occupied by lamellae. This is

analogous to the plot of Rossen and Gauglitz [20] in Figs. 6 and 7. For continuous-gas foam, and at low values of F (roughly below 0.5), gas flows continuously if the actual pressure gradient is less than the minimum value, with no lamella mobilization and no generation of strong foam. For discontinuous-gas foam, resulting from higher values of F , gas flow stops if the pressure gradient is less than the minimum. When the minimum pressure gradient is exceeded, lamellae are mobilized. Thus, Fig. 10(a) maps approximately to the theory of Rossen and Gauglitz [20] without the restrictive assumption of uniform $|\nabla P|$ on the pore network. As Rossen *et al.* [44] conjectured, the two halves of the theory smoothly merge near the percolation threshold. There are two key differences between Fig. 10(a) and the previous theory, however. First, Rossen and Gauglitz consider the onset of mobilization. Here, mobilization, division, and repeated Roof snapoff lead to an asymptotic fluctuation state, where the minimum pressure gradient fluctuates in time around a fixed value. Second, the two branches are much

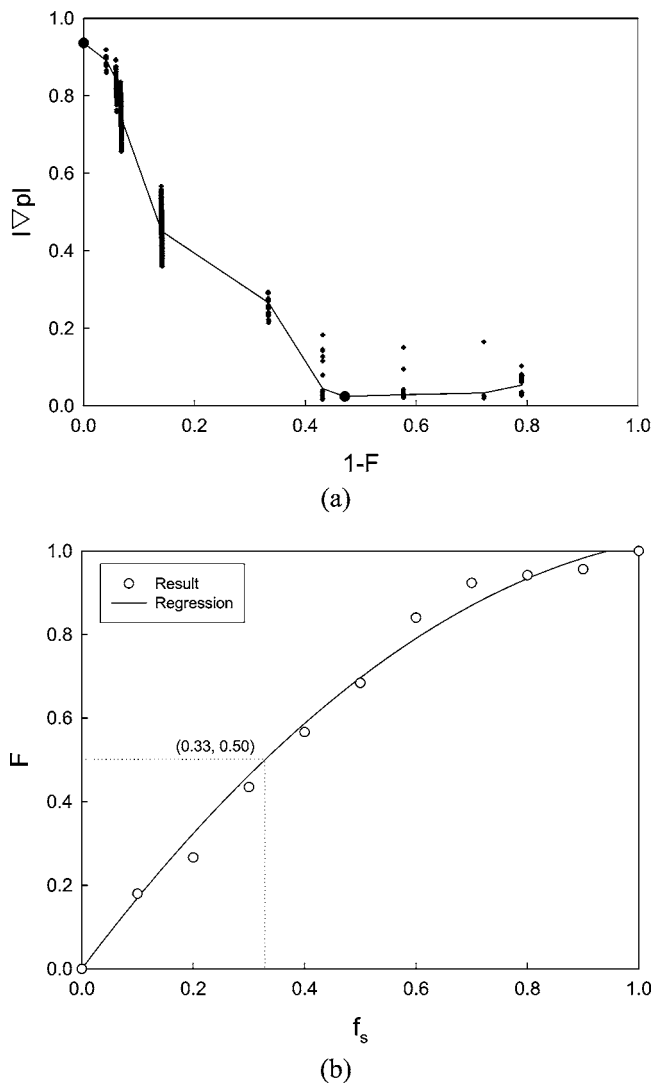


FIG. 10. Foam generation by repetitive snapoff at germination sites and uniform pore size distribution, (a) The minimum pressure gradient as a function of the final fraction of the pore throats occupied by a lamella. Compare to the plot in Figs. 6 and 7 (noting that $F=1-f$, and that here the results correspond to a network with different coordination number than that in Figs. 6 and 7). (b) The final fraction F of throats occupied by lamellae as a function of the snapoff probability. Note the nonlinear relationship and that the percolation threshold for f (0.5 for a square network) is reached at a value of the snapoff probability f_s less than 0.5.

more asymmetric than in the theory: the minimum pressure gradient in the continuous-gas regime is much lower than that in the discontinuous-gas regime, compared to Figs. 6 and 7. (Note also that here the transition between the two regimes occurs approximately at the bond percolation threshold for a square lattice, which is equal to 0.5. In Figs. 6 and 7 the corresponding value was 0.25, equal to the threshold for a Bethe tree with coordination number 5.) Figure 10(b) shows the final lamella fraction as a function of the initial snapoff probability under conditions of incipient lamella mobilization. The curve shows that the final fraction F of pore throats occupied by lamellae rises faster than f_s at small snapoff probabilities, reaches the percolation threshold at f_s

$=0.33$, and approaches unity for f_s well below 1. This behavior reflects the generation of lamellae through additional mechanisms other than snapoff.

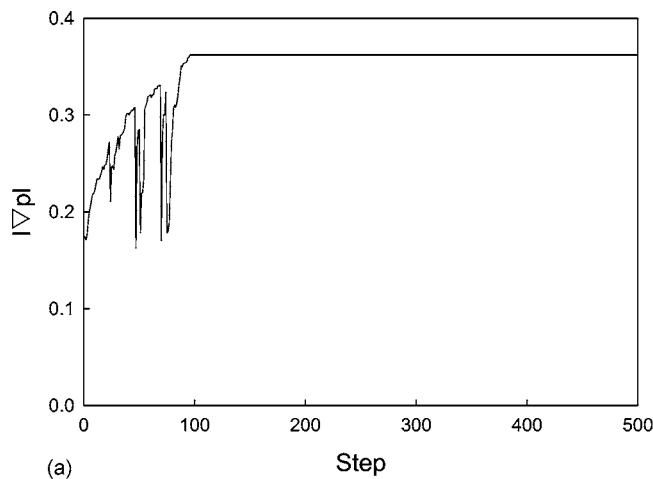
Figures 11 and 12 show corresponding results for the case when the pore-size distribution is unimodal (single pore size). Two features are evident. While the minimum pressure gradient for mobilization fluctuates at short times, as in the case of variable pore sizes, the asymptotic state is not fluctuating, but constant. An initial fluctuating periodic behavior is observed for low values of the snapoff probability, however. The final value of pressure gradient is approximately the same as that for variable pore sizes, the deviation being more pronounced at low values of f_s . It appears that at low values of f_s , the minimum pressure gradient is much higher for a unimodal pore-size distribution than in the case of a uniform distribution between 0.5 and 1.5. We conclude that the disorder in pore size not only alters the nature of the asymptotic state, but in the case of low f_s , it also alters the value of the minimum pressure gradient.

For completeness, we note that if we restrict the generation of snapoff lamellae only to initial drainage of each pore body, the foam thus generated is weak: the gas phase is continuous, regardless of the value of the snapoff probability. Figure 13 shows typical results for two different values of the (initial) snapoff probability ($f_s=0.2$ and 0.7). The asymptotic states reached without lamella creation by repeated Roof snapoff are oscillatory, with a well-defined period of oscillation, e.g., see Fig. 13. This behavior is due to the fact that as lamellae leave the system they are not replaced by new snapoff lamellae, and although new lamellae are generated by lamella division these are not sufficient to block the path of the continuous gas phase and create strong foam. Hence, without allowing for snapoff near the inlet of the medium, triggered by other mechanisms (see section below), repetitive Roof snapoff appears to be necessary for continuous foam regeneration.

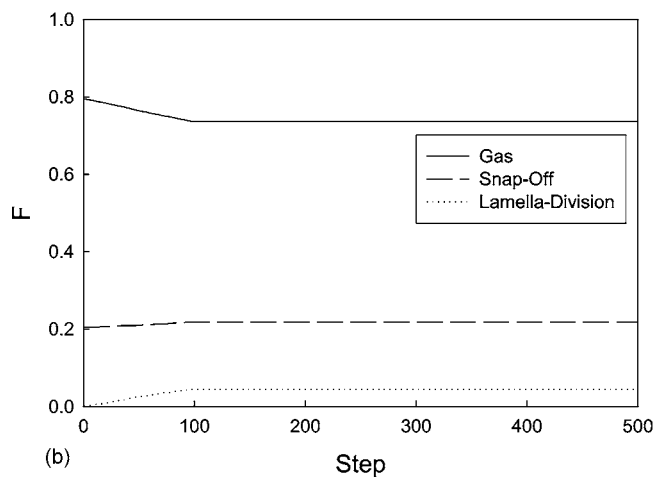
2. Foam rheology

To study foam rheology under the scenario of repetitive Roof snapoff, increasingly higher pressure gradients are applied. In this fashion, the relation between flow rate and pressure drop, and thus the foam rheology, can be determined. We note in advance that the foam texture so obtained is not necessarily the same as that for the state of incipient mobilization.

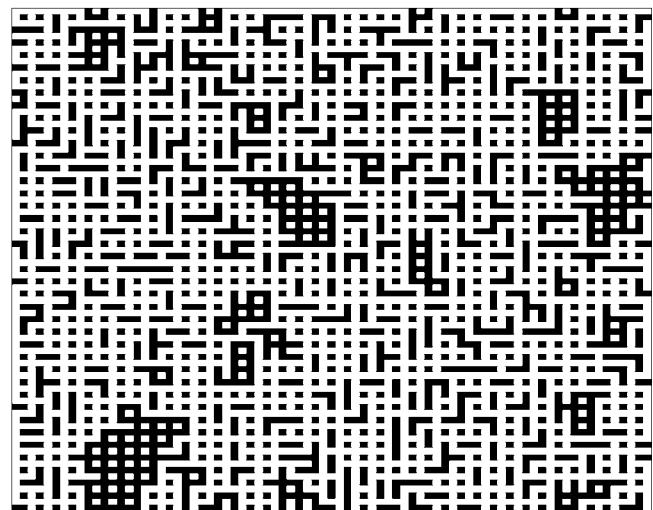
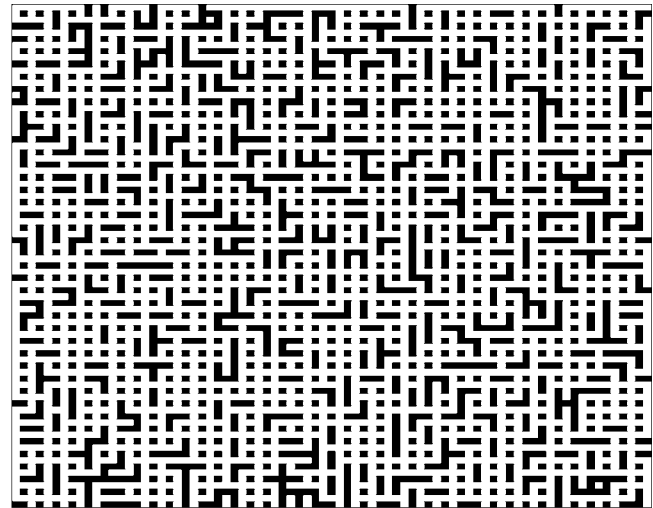
Consider Fig. 8(a) at low snapoff probability, and assume that initially a small pressure gradient is applied. Because of the initially continuous gas phase, at small pressure gradient gas flows without mobilizing any lamellae. Thus, at a sufficiently small pressure drops, the relation between flow rate and pressure drop is linear. On the other hand, if the snapoff probability is higher [e.g., as in Fig. 9(a)], the gas phase is discontinuous from the outset, and no gas flow occurs, unless a minimum pressure gradient is applied to mobilize lamellae along some path (the MTP). If the pressure gradient is continuously increased, e.g., in Fig. 8(a), a threshold of single-lamella mobilization will be reached. Then, lamellae will be mobilized, new lamellae will be generated, and the mobility of the gas phase will decrease. In this sequence, the fluid



(a)



(b)



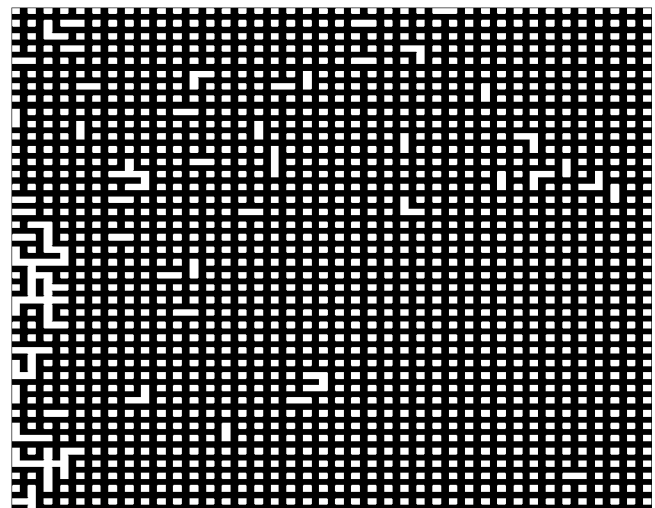
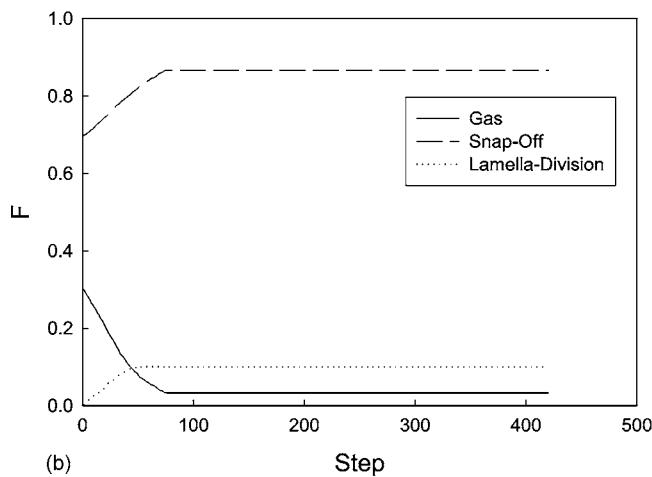
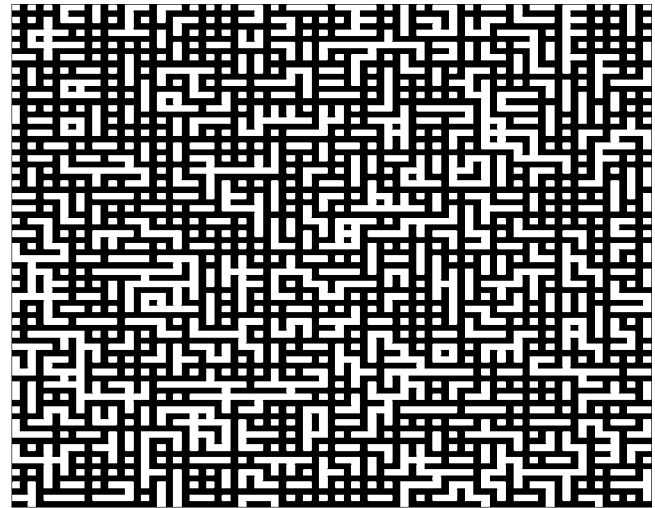
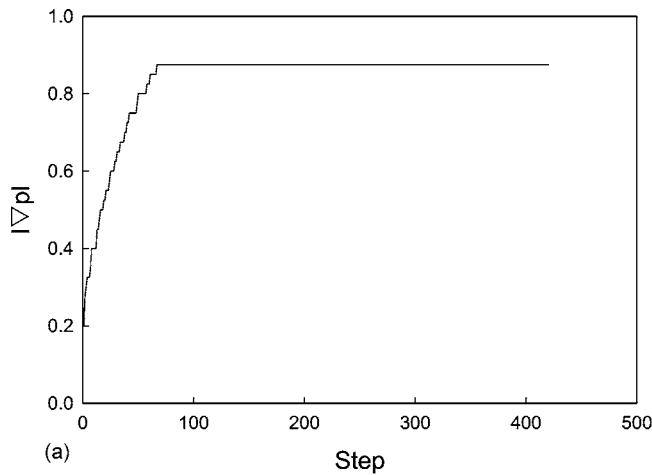
(c)

FIG. 11. Foam generation by repetitive snapoff at germination sites ($f_s=0.2$, unimodal pore-size distribution). (a) The minimum pressure gradient corresponding to the state of incipient mobilization. The gas is continuous in all states. (b) The fraction of pore throats occupied by continuous gas or lamellae of various types. The gas is continuous in all states. (c) Two lamella patterns corresponding to the initial state and one of the final states of (a). The gas is continuous in all states. Gas is white, liquid and rock grains are black.

appears to be shear-thickening behavior (foams are expected to be shear thinning at fixed bubble size, but here the bubble size is decreasing with increasing pressure gradient). We point out that as long as the minimum pressure gradient is monotonically increasing, e.g., as in the early part of Fig. 8(a), the foam remains at the state of incipient mobilization. However, as Fig. 8(a) shows, the minimum pressure gradient decreases after some point. For an applied pressure gradient above this minimum, multiple lamellae, and not only one, will be mobilized. The minimum pressure gradient decreases because mobilized lamellae are moving downstream within the streamtube noted before, with some of them leaving the network completely. Then the gas phase will flow both as a continuous and as a discontinuous phase. The flow rate–pressure drop relation is now a function of time, as lamellae constantly rearrange until the system reaches an asymptotic state.

The flow rate–pressure drop relation resulting from this sequence is shown in Figs. 14 and 15 for two different values

of the snapoff probability ($f_s=0.3$ and 0.7). In the first case, Fig. 14, the gas phase is continuous, and the fluid behaves initially as a Newtonian fluid, as all lamellae are stationary. As the pressure gradient increases, lamellae are being mobilized and at higher values of pressure the gas flows both as a continuous and as a discontinuous phase. In that regime and after the transient rearrangement alluded to above, the rheology of the foam is shear thickening. The results for the case of higher snapoff probability are different, however. For a sufficiently high probability, an increasing number of lamellae must be mobilized before the gas can flow (e.g., see Fig. 9). As these are mobilized, they create lamellae by division, which makes further mobilization even more difficult, unless the pressure is increased further, in which case more lamellae are mobilized and more lamellae are created by division. The final result is that rapidly all throats are filled with lamellae, and the system becomes identical to that of the flow of a uniform Bingham plastic. This is the problem discussed in detail by Chen *et al.* [48]. The corresponding flow velocity–



(c)

FIG. 12. Foam generation by repetitive snapoff at germination sites ($f_s=0.7$, unimodal pore-size distribution). (a) The minimum pressure gradient corresponding to the state of incipient mobilization. The gas is discontinuous in all states. (b) The fraction of pore throats occupied by continuous gas or lamellae of various types. The gas is discontinuous in all states. (c) Two lamella patterns corresponding to the initial state and one of the final states of (a). Gas is white, liquid and rock grains are black. The gas is discontinuous in all states.

pressure drop relationship is identical to that of the flow of a fluid with yield stress (e.g., shown in Fig. 15). This rheology exhibits an aggregate shear-thinning behavior after the onset of flow, although at large pressure gradients it approaches a Newtonian behavior.

B. Case II: Lamella generation due to capillary-pressure fluctuations

The second scenario considered involves the generation of lamellae when the liquid saturation has been reduced to a small value, and the liquid resides in pore corners or in connected films along the pore walls. In this and the following section, we will assume that Roof snapoff generates lamellae only as gas invades a pore body filled with liquid. Subsequent snapoff is assumed here to occur only when the capillary pressure in any throat drops below half of the entry value of that throat.

Implementing this mechanism requires an estimation of the liquid pressure field. While this will be computed in the next section using the pore network, here we will proceed with a simplification, by assuming a uniform liquid pressure gradient along the flow direction: Without loss of generality, we set the liquid pressure at the exit to zero, that at the entrance to a fixed value p_{l0} , and in between to a linear interpolation along the main flow direction. A more elaborate (and accurate) model, by computing the liquid pressure in each throat, is also possible but will be reported in the following section. The gas-phase pressure downstream is set equal to a capillary pressure value p_c , and for the present purposes we assume that the gas viscosity is very small, so that in the absence of lamellae the gas pressure is spatially uniform. For a 2D network of size $L \times L$, a corresponding liquid capillary number can be roughly estimated, if one assumes that the liquid flows in the form of connected corner flows with dimensionless thickness δ . In the following for illustration purposes we will take $\delta=0.1$. The capillary num-

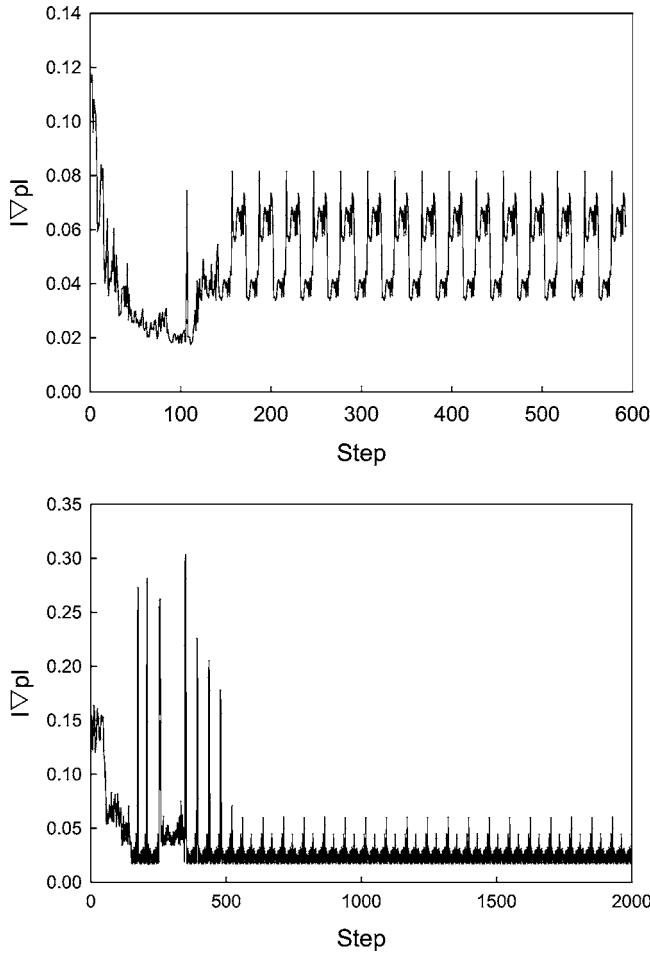


FIG. 13. Foam generation by initial snapoff at germination sites, corresponding to $f_s=0.2$ (top) and 0.7 (bottom). The minimum pressure gradient corresponding to the state of incipient mobilization is shown. The gas is continuous in all states, and very weak foam is observed.

ber is roughly equal to $Ca=4\alpha\delta p_{l0}/L$ where α is a dimensionless parameter that relates permeability to the hydraulic diameter, and it is of the order of 10^{-2} (e.g., see [52]). A sufficient condition for lamella *generation*, in the absence of any lamellae along some path across the network is, in our dimensionless notation,

$$p_c - p_{l0} = p_c - \frac{LCa}{4\alpha\delta} < \frac{1}{4r_{\max}} = \frac{1}{6} = 0.1666, \quad (8)$$

corresponding to a dimensional local capillary pressure of γ/R_{\max} . Equation (8) implies that the capillary pressure is low enough at the inlet to trigger snapoff in any throat. (Recall that pores are uniformly distributed in the range $[0.5, 1.5]$.) For sufficiently large systems, condition (8) is always in effect. Conversely, a sufficient condition for *no generation* is

$$p_c - p_{l0} = p_c - \frac{LCa}{4\alpha\delta} > \frac{1}{4r_{\min}} = \frac{1}{2} = 0.5. \quad (9)$$

If condition (9) applies, there is no lamella (or foam) generation by snapoff. Otherwise, lamellae will be generated, when

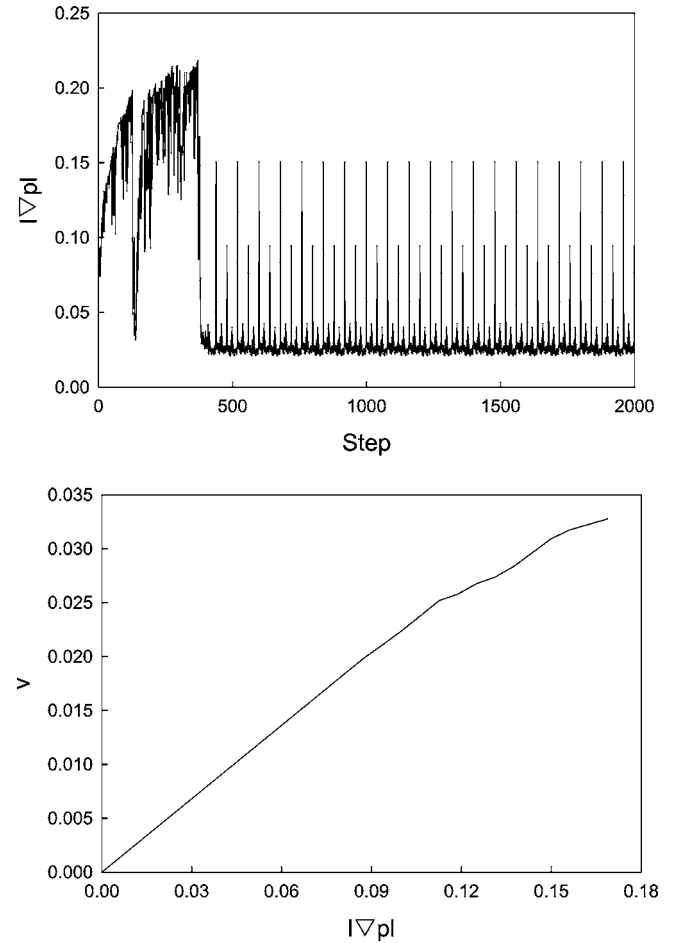


FIG. 14. Foam generation by repetitive snapoff at germination sites corresponding to $f_s=0.3$ and a uniform pore-size distribution. The top panel shows the minimum pressure gradient at conditions of incipient mobilization for the specific f_s value. The bottom panel is a plot of the flow velocity–pressure drop relationship. Because the gas phase is continuous, the fluid behaves initially as Newtonian, with shear-thickening behavior at higher $|\nabla p|$, as lamellae are mobilized and additional lamellae are created by division.

the gas phase is continuous, mostly upstream. The upstream generation follows from the capillary pressure, which, if the gas phase is continuous, is

$$p_g - p_l = p_c - p_{l0} + \frac{x}{L} p_{l0}. \quad (10)$$

In the above interpretation, lamella generation is favored at low capillary pressures (or at a high capillary number for the liquid). Based on this scenario, we determined the state of the foam by proceeding, as in the previous section, either by operating always at the state of minimum pressure gradient (the state of incipient mobilization) or by operating at a pressure gradient above the minimum and seeking the flow rate–pressure drop relation.

1. State of incipient mobilization (minimum pressure gradient)

Figures 16–18 show characteristic results for a 2D pore network and for the scenario in which the state is incipient

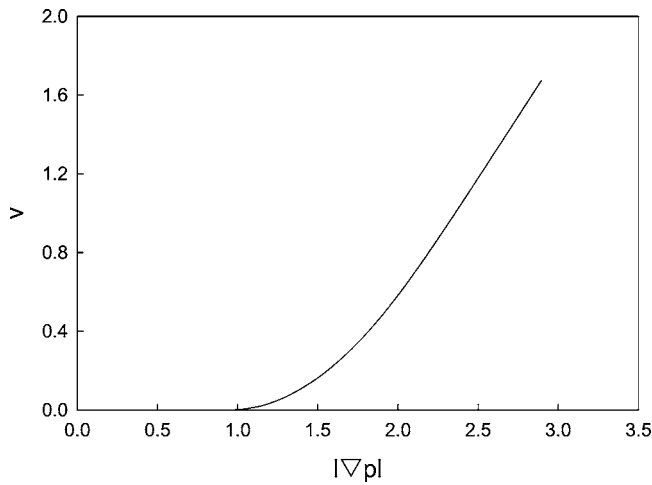


FIG. 15. Foam generation by repetitive snapoff at germination sites corresponding to $f_s=0.7$ and a uniform pore-size distribution. Because of the high snapoff probability, the system rapidly becomes fully occupied by lamellae (through snapoff and lamella division); hence it becomes identical to a Bingham plastic, as discussed by Chen *et al.* [48]. The corresponding flow velocity–pressure drop relationship is identical to that of the flow of a fluid with yield stress. Note difference in scale of $|\nabla p|$ with Fig. 14.

mobilization. Figure 16 shows that the value of the minimum pressure gradient initially fluctuates and ultimately settles into a periodic behavior between two states. The corresponding patterns of the two states are shown in Fig. 17. They correspond either to an open (continuous) gas path, where lamellae are generated due to capillary pressure differences, or to a completely plugged state, where gas is trapped, the

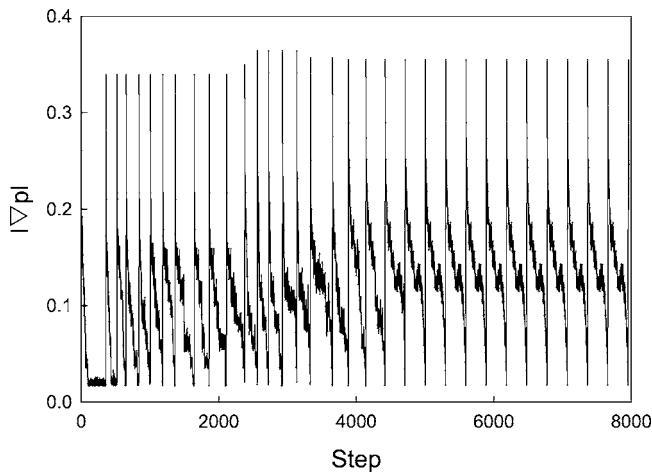


FIG. 16. The minimum pressure gradient corresponding to the state of incipient mobilization, in which lamellae are generated by capillary pressure fluctuations. ($f_s=0.3$, $p_c=5.1677$, $p_{l0}=7.6677$, $Ca=7.677 \times 10^{-4}$, $L=40$). The value fluctuates between two extreme states, one in which the gas has a continuous path (corresponding to a zero value of the minimum pressure gradient) and a state in which the gas is completely discontinuous. In between states correspond to the displacement of lamellae from the blocked paths and the creation of a continuous path. The number of steps corresponds to the number of lamellae moved.

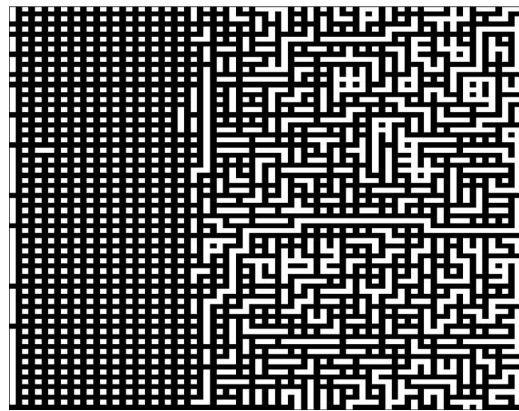
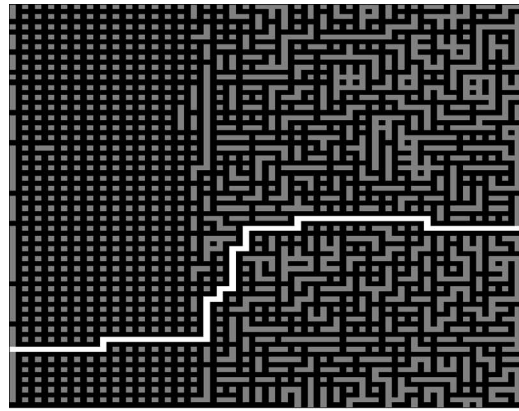


FIG. 17. Lamella patterns corresponding to Fig. 16. The system fluctuates between two extreme states, one in which the gas has a continuous path (shown above as a white line) and a state in which the gas is completely discontinuous. When the first state is reached, the capillary pressure drops and new lamellae are generated in the continuous path. These are advected downstream until a continuous gas path opens. For emphasis, in the top figure gas in the continuous path is white and the remaining gas gray; otherwise, gas is white, liquid and rock grains black.

local capillary pressure is high, and no new lamellae are generated. When in the latter state, lamellae will be mobilized upon consecutive increases in the pressure gradient (recall that by assumption the system is always at the incipient mobilization state): then lamellae will be advected downstream and eventually open a continuous gas path across the medium. This will be followed by the rapid drop of the gas pressure, and the subsequent generation of lamellae, via the capillary-pressure mechanism. (In reality, of course, this change in the capillary pressure, assumed to be instantaneous here, takes a certain time period, as liquid needs to imbibe in response to the change in the local pressure.)

The cycle is then repeated and involves a number of intermediate states in-between. As the variable $p_c - p_{l0}$ decreases, the density of new lamellae generated increases, provided that condition (8) is satisfied. The plot of the maximum value in $|\nabla p_{\min}|$ (namely, of the highest value of the quantity in Fig. 16), is shown in Fig. 18, as a function of $p_c - p_{l0}$ and of the initial snapoff probability f_s . As expected, it increases as $p_c - p_{l0}$ decreases, ultimately reaching a limiting value at sufficiently negative values of the difference $p_c - p_{l0}$. This

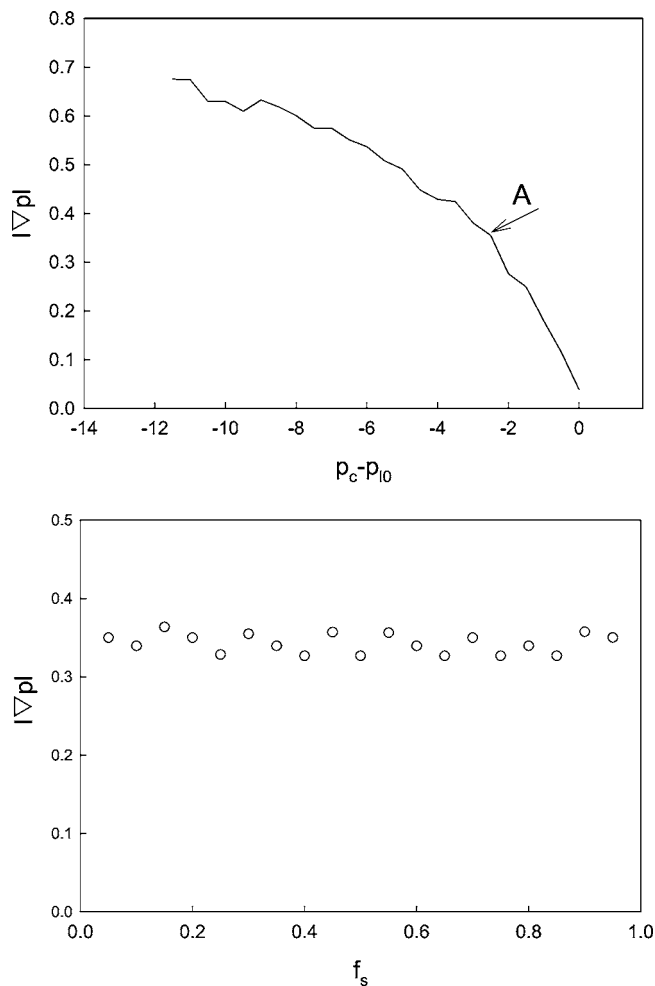


FIG. 18. The minimum pressure gradient at incipient mobilization corresponding to the maximum value of the fluctuating cycle between the states, as a function of the parameter $p_c - p_{l0}$ (for $f_s = 0.3$), at the top panel, and of the initial snapoff probability f_s (for $p_c - p_{l0} = -2.5$ corresponding to point A in the top panel) at the bottom panel.

plateau (not shown in the figure) is equal to 0.96 and corresponds to the limit where all throats contain lamellae. The effect of the initial snapoff probability f_s , is not significant, however. Apparently, as long as there is significant potential for lamellae generation by capillary-pressure fluctuations, the initial snapoff probability is not an important factor in the ultimate behavior of the system.

To summarize, following the initial snapoff, a discontinuous gas is created. Lamellae are advected downstream (and leave the system), until a continuous path for the gas opens up, at which time the capillary pressure mechanism comes into effect, and new lamellae form in the open path. This leads to the disconnection of the gas phase, and the repetition of the above cycle. We expect, therefore, the system to operate in a fluctuating state, between a state of low pressure drop, where the gas phase is continuous and the number of lamellae minimal, and a state of high pressure drop, where the gas phase is discontinuous and the number of lamellae large, but slowly decreasing, as the lamellae are convected downstream. This gradual depletion of lamellae leads ulti-

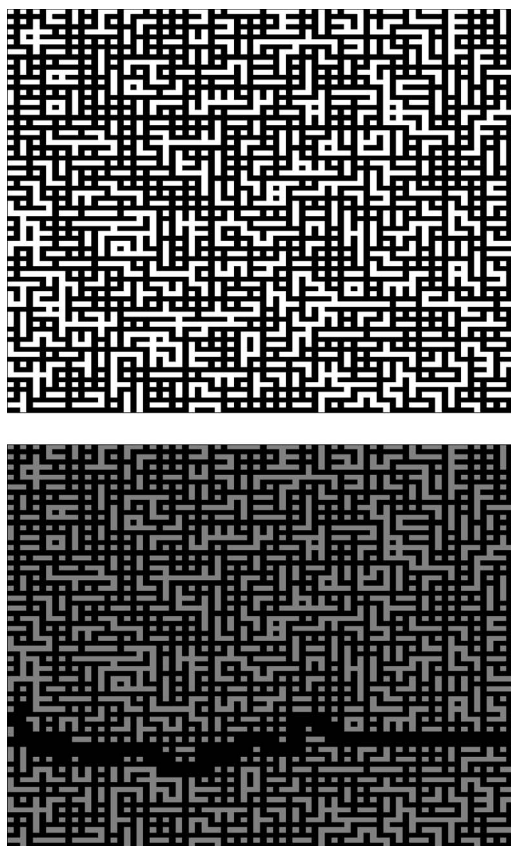


FIG. 19. Lamellae patterns corresponding to two different states under the application of a constant pressure drop and for the scenario in which lamellae are generated by capillary pressure fluctuations ($f_s = 0.7$, $p_c = 5.1677$, $p_{l0} = 7.6677$, $|\nabla p| = 0.17$, $Ca = 6.8 \times 10^{-4}$). The system fluctuates between two extreme states, one in which the gas has a continuous path (shown in the bottom figure as a white line) and a state in which the gas is completely discontinuous (top figure, corresponding to the initial state, but which is also similar to one of the two extremes of the asymptotic state). Gas is gray or white, liquid and rock grains black.

mately to the opening of a continuous path and to the generation of lamellae upstream, following which the cycle continues.

2. Foam rheology

Consider, next, the case in which the applied pressure gradient is above the minimum mobilization pressure. Contrary to the case of a Newtonian, or even of a Bingham fluid, this does not lead to a steady state. For a given value of $(p_c - p_i)$, we fixed the applied pressure drop to a constant value above the corresponding value in Fig. 18 and kept it constant thereafter. Figure 19 shows two different snapshots of the lamella pattern, illustrating the mechanism discussed. During this process, and until an open path develops, the flow rate increases with time (Fig. 20) in a fluctuating manner, until a continuous-gas-phase path opens. Then, new lamellae are generated and the cycle commences anew. Evidently, in this case the time dependence of the flow rate precludes the use of a constant mobility for the foam. Note that in Fig. 20 time is made dimensionless by dividing by the

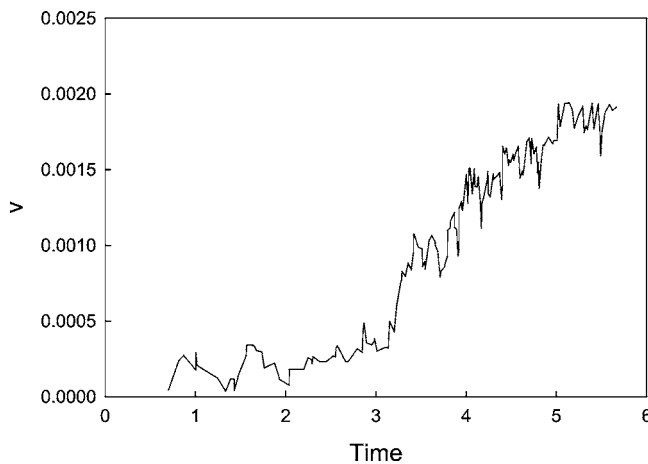


FIG. 20. The gas flow rate as a function of time for the process of Fig. 19, namely, under the application of a constant pressure drop and for the scenario in which lamellae are generated by capillary-pressure fluctuations. One complete cycle is shown. At the end of the cycle, a continuous gas path opens, new lamellae are generated by falling capillary pressure and the process is repeated. The increasing flow rate as a function of time results from the mobilization and the advection downstream of lamellae in a pore network in which the gas phase is disconnected ($f_s=0.7$, $p_c=5.1677$, $p_{l0}=7.6677$, $|\nabla p|=0.17$, $Ca=6.8 \times 10^{-4}$).

characteristic time, $t^* = 2\mu_g R^* L^2 / \gamma \Delta p$, which is the time it would take for a passive tracer to be advected across the lattice, assuming a unimodal pore-size distribution, and based on the same applied pressure difference.

These figures illustrate two important results. First, snapoff of lamellae near the inlet to the medium can replenish the supply of lamellae after mobilization and the displacement of lamellae downstream. Mobilization and division, combined with snapoff driven by episodically low p_c near the inlet, can maintain foam at a sort of fluctuating state. Therefore, repeated Roof snapoff, governed by the pore throat-body geometry, is not necessary for steady foam regeneration. Second, the pressure drop fluctuates around this steady state. This confirms a common observation that fluctuations are an inherent part of the regeneration process for foam.

The fluctuations shown here are related but not identical to those cited by Rossen [15]. Those fluctuations arise from the changes in shape and curvature of a fixed population of lamellae moving through the converging-diverging geometry of pores. Here, they arise from the changing population of lamellae: the creation of new lamellae by snapoff and their subsequent displacement out of the region of interest. This process represents an additional mechanism of snapoff and foam generation.

C. Case III: Lamella generation during immiscible displacement

The third and final case will focus on the formation of foam during the process of gas invasion and displacement of an initially liquid-occupied medium. This scenario models foam generation during the simultaneous steady-state flow of

liquid and gas. Surfactant-laden liquid flows at a constant rate as a continuous phase by fully occupying pores (rather than by residing in the corners of pores or as macroscopic films along pore walls, as discussed previously). The liquid flow rate is fixed and sets the capillary number. Gas is simultaneously injected at a constant rate. Lamellae are generated as the gas-phase saturation (volume fraction) is increased through mechanisms of Roof snapoff (operating only once per germination site), leave behind, and lamella division. A key objective is to determine the mobility (or relative permeability) of the foam as a function of the liquid saturation, the capillary number, and other parameters. Again, no lamella destruction is considered.

To simulate the process, we first used an invasion percolation algorithm [50] to find a continuous path for the gas phase, as in the conventional drainage process. During this process, lamellae are created by snapoff, at probability f_s , and by leave behind. Recall that f_s represents the probability that a given throat-body combination has the right geometry for Roof snapoff [27]. As before, these probabilities are assigned randomly, independently of the throat radius. In contrast to case I, however, Roof snapoff happens only once per throat, during the drainage of the pore by gas. Following the gas breakthrough, a constant liquid velocity (hence a constant capillary number) is imposed on the liquid. Under these conditions, the liquid-gas system will seek a steady state. The corresponding pressure profile in the gas can be readily determined, based on the assumption of a spatially uniform capillary pressure between gas and liquid. If the resulting overall pressure difference across a path of lamellae is sufficiently high (as determined using IPM), these lamellae will be mobilized. They will move, divide, and create other lamellae, as appropriate, until finally a steady state is reached, in which no further mobilization occurs. When this state is reached, the gas flow rate and the gas mobility, corresponding to the given capillary number, are computed.

We also need to note the following rules used in the calculations. If several lamellae are moving, the first lamella to divide is the one requiring the minimum amount of time to move to a neighboring throat. Lamellae may also be divided into two or more, depending on the occupancy of throats and pore bodies by gas or liquid. Lamellae can be generated by division only in downstream throats. Before a steady state is reached, the first gas-liquid interface to advance is taken as that with the maximum value of the dimensionless pressure difference

$$\max \left(p_g - p_l - \frac{1}{2r} \right).$$

The advance of this interface leads to a reduction of the liquid saturation. In the process, new snapoff and/or leave-behind lamellae may be created. As in the previous scenarios, destruction of lamellae is not accounted for. Lamellae leave the region of interest by advection, but not by destruction.

Figure 21 shows patterns of lamella distribution in a 100×100 , 2D pore network with $Ca=0.01$, and at different values of liquid saturation. Until gas breakthrough (top panel of Fig. 21) lamellae were generated by snapoff but not by

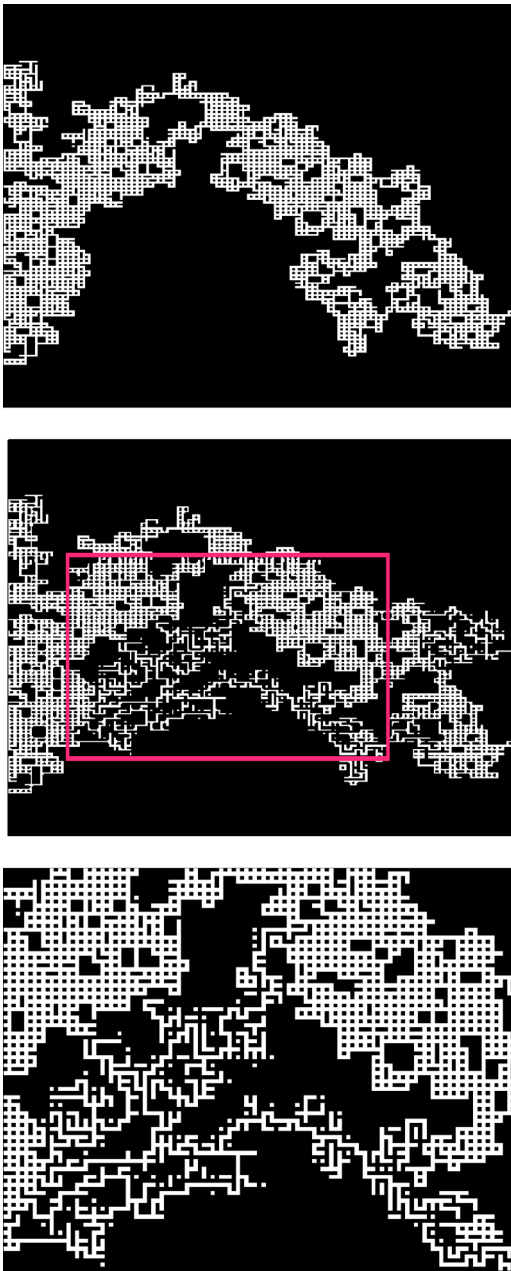


FIG. 21. (Color online) Sequence of patterns illustrating liquid displacement in a 2D network and the creation of lamellae. The top panel shows the conditions at breakthrough, the middle panel conditions at a higher value of the applied pressure drop. The bottom panel is an enlargement of a region in the middle panel showing a number of lamellae generated by snapoff and leave-behind mechanisms. The liquid flows at a constant rate corresponding to $Ca = 10^{-2}$. Gas is white, liquid and rock grains are black. Extensive lamella formation by leave behind occurs as the liquid is being displaced.

leave behind. This corresponds to initial drainage with no surfactant present. After gas breakthrough, surfactant is assumed to be present, and, in the subsequent invasion of gas-liquid interfaces in the liquid and the liquid displacement, new leave-behind and snapoff lamellae are generated. The new snapoff lamellae may isolate the gas-liquid interface

from the bulk gas. This type of interface will not be moved, unless the corresponding lamellae can be mobilized (determined using IPM). As the gas pressure difference increases, the liquid saturation decreases, at constant capillary number, and the relative mobility of the foam, namely, its relative permeability, can be computed as a function of the liquid saturation.

Figure 22 shows results on the fraction of pores occupied by various lamella types, the relative permeabilities of the two phases, and the foam rheology obtained for a $20 \times 20 \times 20$ pore network, for the parameter values $f_s = 0.1$, $M = 100$, and $Ca = 0.001$. M is the ratio of viscosities between liquid and gas (without foam). Because of the small snapoff probability in Fig. 22, the gas phase remains continuous throughout. As the gas-phase pressure increases, the liquid saturation decreases, and the number of lamellae in the gas increases, mostly through the leave-behind mechanism. (The significant number of leave-behind lamellae may be due to the larger coordination number in the 3D network [2].) Lamella creation in the gas phase causes the relative permeability of the gas to be much smaller than in the absence of lamellae, under the same conditions in Ca and M . With a continuous gas path always available, the rheology of the gas remains approximately Newtonian [i.e., the flow velocity remains roughly proportional to the pressure drop; see Fig. 22(c)]. An increase in the pressure drop leads to more lamellae being mobilized, but also to the displacement of the liquid and the potential opening of new flow paths. Again, we point out that the gas phase was assumed Newtonian, with no shear-thinning features in the presence of lamellae. The relative permeability of the liquid remains very similar to that for a typical immiscible displacement and is unaffected by the presence of foam. We note that in Fig. 22(c) the velocity on the vertical axis is a dimensionless expression of the superficial velocity V ,

$$\nu = \frac{2\mu_g V}{\phi\gamma} \quad (11)$$

where ϕ is the porosity. Alternatively, ν is the relative velocity compared to the velocity the gas would have if it flowed in a porous medium consisting of identical pores of size R^* under a pressure gradient equal to $4\gamma/R^*$.

The effect of the capillary number is shown in Fig. 23, under the same conditions as Fig. 22, but where the liquid flow rate is now increased by one order of magnitude. The plots corresponding to the fraction of lamellae generated and the flow rate–pressure drop relationship are similar to Fig. 22, and not shown. The most interesting new feature is that the relative mobility of the gas is now higher. This is consistent with the interpretation above, namely, the fact that at a higher pressure difference more lamellae are mobilized, with a resulting larger flow rate in the continuous path of the gas phase. The increase in the relative permeability reflects the well-known relative-permeability effect of the capillary number for any immiscible displacements [53]. That is, much as sufficient pressure gradient can mobilize residual phase and increase relative permeabilities in conventional two-phase flow, sufficient pressure gradient can displace lamellae in foam flow.

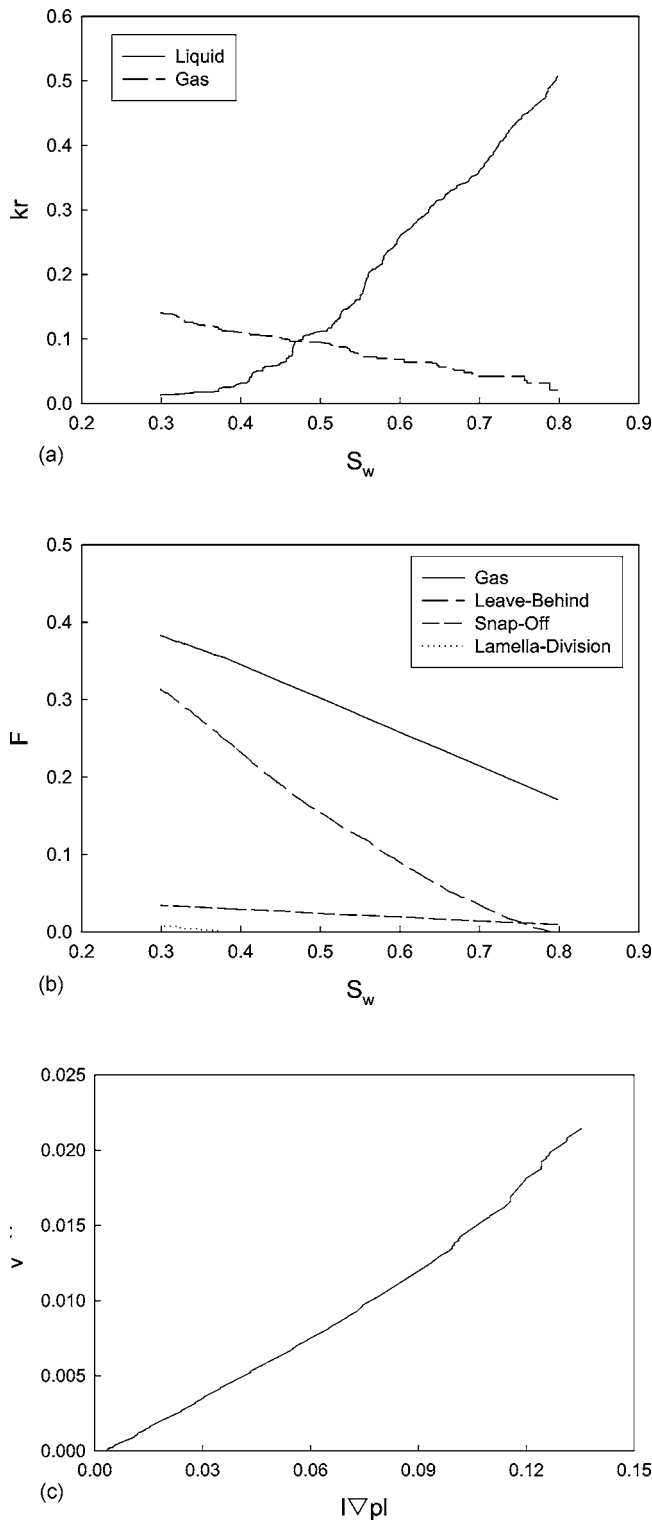


FIG. 22. Steady-state results corresponding to foam generation during the displacement of liquid by gas, with snapoff probability $f_s=0.1$, $M=100$, and $Ca=10^{-3}$. (a) Relative permeabilities (k_r) as functions of S_w . (b) The fraction F of pore throats containing gas without lamellae, leave-behind lamellae, snapoff lamellae, and lamellae created by division as functions of S_w . (c) Flow velocity as a function of the applied pressure drop. The liquid saturation S_w falls as $|\nabla P|$ rises.

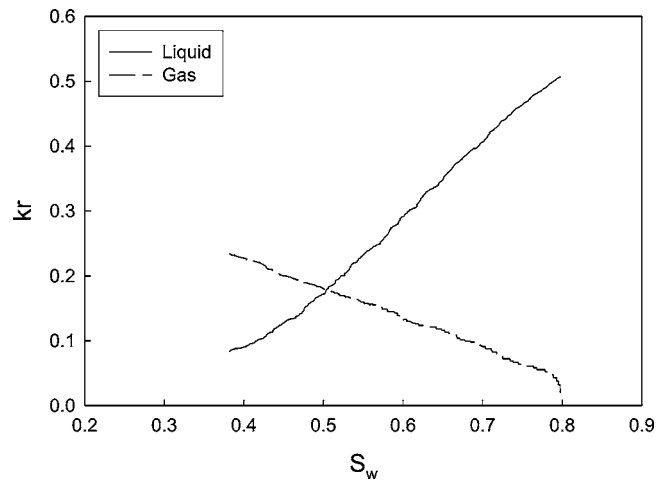


FIG. 23. Steady-state relative permeability results corresponding to foam generation during the displacement of liquid by gas, with snapoff probability $f_s=0.1$, $M=100$, and $Ca=10^{-2}$. The increase in the liquid rate (capillary number) leads to increased relative permeabilities in both fluids.

Under the same conditions an increase in the snapoff probability fraction (Fig. 24, with $f_s=0.7$), leads to a corresponding increase in the lamellae fraction and a decrease in the relative mobility of the gas. Qualitatively, the features of the generated foam are much more pronounced than previously, however. First, the relative permeability of the gas phase is much lower. More importantly, the gas phase is disconnected and cannot be mobilized until after the liquid saturation has been reduced to a critical value, the liquid having retreated to narrow throats. Otherwise, the gas is trapped and flow does not occur. The corresponding critical gas saturation is equal to about 0.65 in this case. Second, there exists a minimum pressure drop for the mobilization of the gas phase, associated with the critical saturation, endowing features of a yield-stress fluid. This value is a function of the capillary number, with higher capillary numbers leading to an earlier onset of mobilization. Thus, at higher snapoff probabilities, and given a capillary number, foam does not flow until the applied pressure gradient, and hence the gas saturation, exceeds a certain value. The dependence of the critical gas saturation (and of the minimum pressure gradient) on the capillary number and the snapoff probability is a subject of an ongoing investigation. The resulting rheology [Fig. 24(b)] is that of a yield-stress fluid, where a minimum pressure gradient is necessary for the onset of gas flow. Following mobilization, the system ultimately reaches a steady state, in which a continuous path is available, because at that point the flow rate increases rapidly, and the flow velocity–pressure drop relationship becomes almost discontinuous. The fraction of lamellae generated by snapoff [Fig. 24(c)] is considerably larger than in the case of a low snapoff probability, as expected, although the number generated by leave behind is about the same. Nonetheless, without a mechanism for lamella creation near the inlet, as lamellae are mobilized eventually a continuous gas path forms.

IV. EXTENSIONS

At this stage the network model is suited to hypothesis testing (e.g., does steady foam generation require Roof

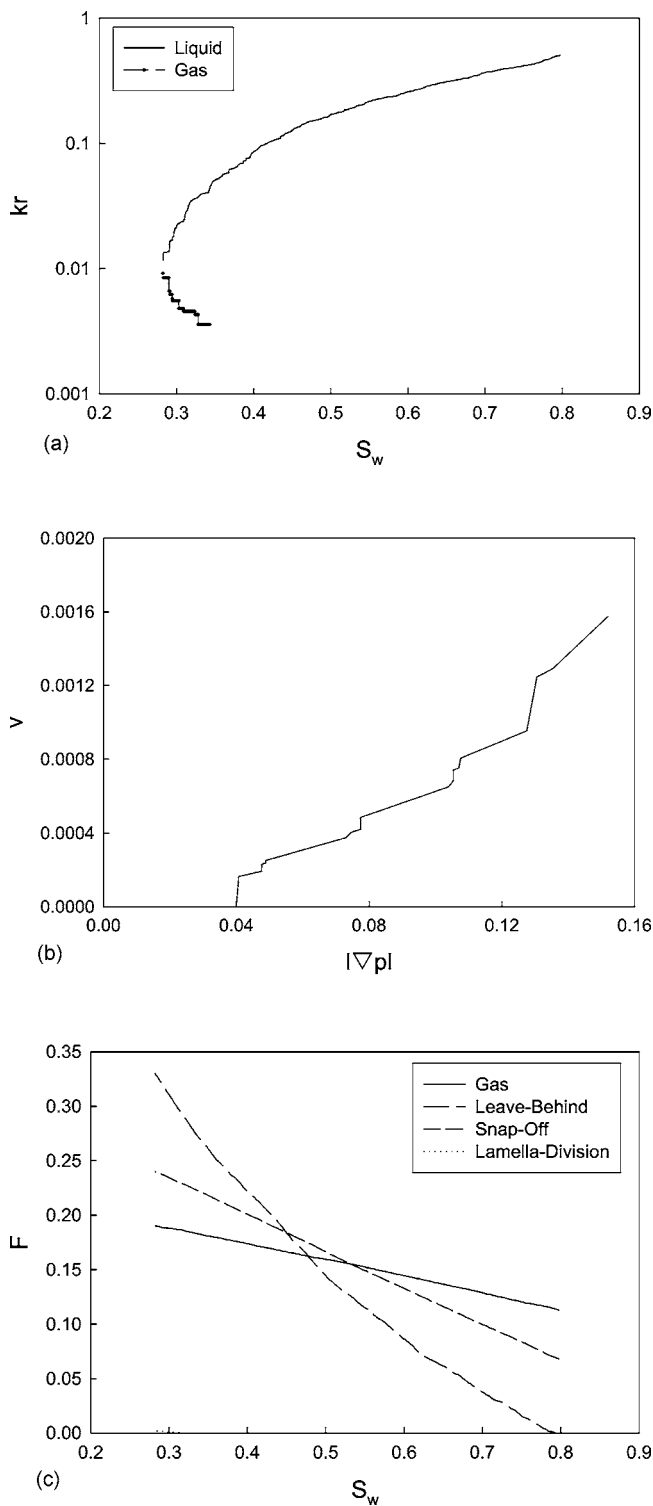


FIG. 24. Steady-state results corresponding to foam generation during the displacement of liquid by gas, with snapoff probability $f_s=0.7$, $M=100$, and $Ca=10^{-3}$. (a) Relative permeabilities (k_r) as functions of S_w . (b) The flow velocity as a function of the applied pressure drop. (c) The fraction F of pore throats containing gas without lamellae, leave-behind lamellae, snapoff lamellae, and lamellae created by division as functions of S_w . Note the existence of a critical gas saturation (and a critical pressure gradient), below which the gas relative permeability vanishes.

snapoff? Is the model of Rossen and Gauglitz [20] fundamentally inconsistent at the percolation threshold?), as well as for providing insights into microscopic processes (e.g., the oscillatory or chaotic nature of foam mobilization and flow). To create a complete network model for foam flow, the following extensions would be needed.

(1) More realistic portrayal of gas viscosity, incorporating a $-1/3$ power of gas velocity [11] and coupling between capillary pressure and gas viscosity [54].

(2) Increased 3D network size, while modeling flow of wetting fluid in corners and along walls of pores filled with nonwetting fluid. The latter is crucial to accurate modeling of water relative permeability at low water saturations.

(3) Incorporation of mechanisms of foam destruction, especially foam collapse in the vicinity of the limiting capillary pressure [25].

Once all mechanisms are accounted for, it still remains to express the results in terms of variables used in mechanistic foam simulation [10,13,14,26,35,36,42,55]: expressions for rate of change of lamella density in the network, and gas mobility as a function of lamella density, water saturation, and gas velocity. It is possible that a complete network model might show that one cannot represent gas mobility without the spatial information retained in the network model itself.

V. CONCLUSIONS

In this paper we used a pore-network model to study various scenarios for foam formation and propagation in porous media. They all included appropriate pore-level mechanisms of lamella formation through snapoff, lamella division following lamella mobilization, and leave behind following the displacement of gas-liquid interfaces. Three different scenarios were modeled: one in which Roof snapoff occurs repeatedly at specific, randomly distributed germination sites; another in which the lamellae are generated by capillary-pressure fluctuations, during the simultaneous flow of gas and liquid, with liquid flow in pore corners or along pore walls modeled schematically; and a third corresponding to drainage displacement, in which liquid and gas flow at steady state and lamellae are generated by snapoff and leave behind at advancing interfaces. Because foam is always in dynamic equilibrium, a specific foam state depends on the path by which it was reached. Two different cases were examined in each scenario: a case of incipient mobilization, in which the minimum pressure gradient to mobilize a single lamella was computed, and a state in which a specific pressure gradient is applied, and in which the flow rate–pressure drop relation was sought. Clearly, the rheology of the foam depends greatly on how these states were reached.

Because of the intricate dynamic equilibrium involved in the flow of the gas and the liquid, and the attendant mobilization of a multitude of lamellae, foam properties were found to be fluctuating, in some cases with a well-defined period and in others in an apparently random manner. When lamellae form by capillary-pressure fluctuations or by repetitive snapoff, the asymptotic state is dynamic. When a steady state is reached, it does not involve mobilization or genera-

tion of lamellae (except for an ideal case of unimodal pore-size distribution), in which case the gas flows as either a Newtonian or a Bingham fluid, but with reduced mobility. In this relatively weak foam case the relative permeability as a function of saturation can be computed.

Our study shows that strong foam generation by lamella mobilization and division and capillary fluctuations is possible without the necessity of repetitive Roof snapoff. Minimum pressure gradient calculations using the latter led to results qualitatively similar to the theory of Rossen and Gauglitz [20] without their assumption of a uniform $|\nabla p|$ in the pore network. The methodology proposed in this work can be used to explore additional properties of foam generation and propagation in porous media.

This work focused only on foam-generation mechanisms, and did not include lamella destruction, e.g., by coalescence or by conditions of exceedingly low liquid saturations, under which lamellae collapse. In addition, we only discussed ther-

modynamic and flow properties, such as the final density of lamellae generated in each scenario, minimum pressure gradients, etc. For conventional simulation models, rates of generation and destruction, often related to the flow velocity, are needed. Finally, we did not account for a commonly assumed feature, namely, that flow of a gas bubble in a porous medium in the presence of liquid films along walls has a shear-thinning behavior, and not the Newtonian behavior assumed here. Regardless of these limitations, we believe that the present study has provided significant insights on the pore-level dynamics of foam formation in porous media.

ACKNOWLEDGMENT

One of the authors (W.R.R.) would like to acknowledge the support of the National Petroleum Technology Office of the U.S. Department of Energy, through Contract No. DE-FC26-01BC15318.

-
- [1] *Foams: Fundamentals and Applications in the Petroleum Industry*, edited by L. L. Schramm, ACS Advances in Chemistry Series No. 242 (American Chemical Society, Washington, DC, 1994).
- [2] W. R. Rossen, in *Foams: Theory, Measurements and Applications*, edited by R. K. Prud'homme and S. Khan (Marcel Dekker, New York, 1996).
- [3] N. Terdre, *Offshore* **63**, 70 (2003).
- [4] R. D. Gdanski, *Oil Gas J.* **91**, 85 (1993).
- [5] L. Cheng, S. I. Kam, M. Delshad, and W. R. Rossen, in *Proceedings of the SPE European Formation Damage Symposium*, The Hague, 2001 (unpublished), Paper SPE 68916.
- [6] G. J. Hirasaki, R. E. Jackson, M. Jin, J. B. Lawson, J. Londergan, H. Meinardus, C. A. Miller, G. A. Pope, R. Szafranski, and D. Tanzil, in *NAPL Removal: Surfactants, Foams, and Micromulsions*, edited by S. Fiorenza, C. A. Miller, C. L. Oubre, and C. H. Ward (Lewis Publishers, Boca Raton, FL, 2000).
- [7] G. G. Bernard, L. W. Holm, and W. L. Jacobs, *SPEJ* **2**, 195 (1965).
- [8] J. M. Sanchez and R. S. Schechter, *J. Pet. Sci. Eng.* **3**, 185 (1989).
- [9] A. S. de Vries and K. Wit, *SPERE* **6**, 185 (1990).
- [10] F. Friedmann, W. H. Chen, and P. A. Gauglitz, *SPERE* **7**, 37 (1991).
- [11] G. J. Hirasaki and J. B. Lawson, *SPEJ* **22**, 176 (1985).
- [12] A. H. Falls, J. J. Musters, and J. Ratulowski, *SPERE* **5**, 155 (1989).
- [13] A. H. Falls, G. J. Hirasaki, T. W. Patzek, P. A. Gauglitz, D. D. Miller, and J. Ratulowski, *SPERE* **4**, 884 (1988).
- [14] A. R. Kovscek and C. J. Radke, in *Foams: Fundamentals and Applications in the Petroleum Industry* (Ref. [2]).
- [15] W. R. Rossen, *J. Colloid Interface Sci.* **136**, 1 (1990).
- [16] W. R. Rossen, *J. Colloid Interface Sci.* **136**, 17 (1990).
- [17] W. R. Rossen, *J. Colloid Interface Sci.* **136**, 38 (1990).
- [18] W. R. Rossen, *J. Colloid Interface Sci.* **139**, 457 (1990).
- [19] Q. Xu and W. R. Rossen, *Colloids Surf., A* **216**, 175 (2003).
- [20] W. R. Rossen and P. A. Gauglitz, *AIChE J.* **36**, 1176 (1990).
- [21] S. I. Chou, in *Proceedings of the SPE/DOE Symposium on Enhanced Oil Recovery*, Tulsa, OK, 1990 (unpublished), Paper SPE 20239.
- [22] C. J. Radke and J. V. Gillis, in *Proceedings of the SPE Annual Technical Conference and Exhibition*, New Orleans, LA, 1990 (unpublished), Paper SPE 20519.
- [23] Q. Nguyen, Ph.D. thesis, Delft University of Technology, 2004 (unpublished).
- [24] G. Q. Tang and A. R. Kovscek, in *Proceedings of the SPE Annual Technical Conference and Exhibition*, Houston, TX, 2004 (unpublished), Paper SPE 90142.
- [25] Z. I. Khatib, G. J. Hirasaki, and A. H. Falls, *SPERE* **4**, 919 (1988).
- [26] H. J. Bertin, M. Y. Quintard, and L. M. Castanier, *SPEJ* **3**, 356 (1998).
- [27] T. C. Ransohoff and C. J. Radke, *SPERE* **4**, 573 (1988).
- [28] K. T. Chambers and C. J. Radke, in *Interfacial Phenomena in Oil Recovery*, edited by N. R. Morrow (Marcel Dekker, New York, 1990).
- [29] D. Tanzil, G. J. Hirasaki, and C. A. Miller, in *Proceedings of the SPE/DOE Symposium on Improved Oil Recovery*, Tulsa, OK, 2002 (unpublished), Paper SPE 75176.
- [30] P. A. Gauglitz, F. Friedmann, S. I. Kam, and W. R. Rossen, *Chem. Eng. Sci.* **57**, 4037 (2002).
- [31] S. I. Kam and W. R. Rossen, *SPEJ* **8**, 417 (Dec. 2003).
- [32] S. I. Kam, Q. Li, Q. P. Nguyen, and W. R. Rossen, in *Proceedings of the SPE Annual Technical Conference and Exhibition*, Houston, TX, 2004 (unpublished), Paper SPE 90938.
- [33] W. R. Rossen, *Colloids Surf., A* **225**, 1 (2003).
- [34] J. G. Roof, *SPEJ* **7**, 85 (1970).
- [35] A. R. Kovscek, T. W. Patzek, and C. J. Radke, *Chem. Eng. Sci.* **50**, 3783 (1995).
- [36] A. R. Kovscek, T. W. Patzek, and C. J. Radke, *SPEJ* **2**, 511 (1997).
- [37] T. J. Myers and C. J. Radke, *Ind. Eng. Chem. Res.* **39**, 2725 (2000).

- [38] J. V. Gillis and C. J. Radke, in *Proceedings of the SPE Annual Technical Conference and Exhibition*, New Orleans, LA, 1990 (unpublished), Paper SPE 20519.
- [39] L. W. Holm, SPEJ **5**, 359 (1968).
- [40] S. H. Yang and R. L. Reed, in *Proceedings of the SPE Annual Technical Conference and Exhibition*, San Antonio, TX, 1989 (unpublished), Paper SPE 19689.
- [41] J. M. Sanchez and R. S. Schechter, J. Pet. Sci. Eng. **3**, 185 (1989).
- [42] D. Veeningen, P. L. J. Zitha, and C. P. J. W. van Kruijsdijk, in *Proceedings of the European Formation Damage Symposium*, The Hague, 1997 (unpublished), Paper SPE 38197.
- [43] H. Kharabaf and Y. C. Yortsos, SPEJ **3**, 42 (1998).
- [44] W. R. Rossen, J. Shi, and S. C. Zeilinger, AIChE J. **40**, 1082 (1994).
- [45] W. R. Rossen, J. Phys. A **24**, 5155 (1991).
- [46] R. Pike and H. E. Stanley, J. Phys. A **14**, L169 (1981).
- [47] M. J. Blunt, M. D. Jackson, M. Piri, and P. H. Valvatne, Adv. Water Resour. **25**, 1069 (2002).
- [48] M. Chen, W. R. Rossen, and Y. C. Yortsos, Chem. Eng. Sci. **60**, 4183 (2005).
- [49] H. Kharabaf and Y. C. Yortsos, Phys. Rev. E **55**, 7177 (1997).
- [50] J. Feder, *Fractals* (Plenum, New York, 1988).
- [51] M. Chen, Ph.D. thesis, University of Southern California, 2004 (unpublished).
- [52] A. Yiotis, A. Bountouvis, A. K. Stubos, I. N. Tsimpanogiannis, and Y. C. Yortsos, AIChE J. **50**, 2721 (2004).
- [53] L. W. Lake, *Enhanced Oil Recovery* (Prentice-Hall, Upper Saddle River, NJ, 1989).
- [54] J. S. Kim, Y. Dong, and W. R. Rossen, SPEJ **8**, (to be published).
- [55] S. I. Kam and W. R. Rossen, SPEJ **8**, 417 (2003).